THESIS FOR THE DEGREE OF LICENTIATE OF ENGINEERING

High-Temperature Corrosion Chemistry in Oxy-Fuel Combustion

THOMAS EKVALL

Department of Energy and Environment

CHALMERS UNIVERSITY OF TECHNOLOGY

Gothenburg, Sweden 2014

High-Temperature Corrosion Chemistry in Oxy-Fuel Combustion

THOMAS EKVALL

Department of Energy and Environment
Chalmers University of Technology
SE-412 96 Gothenburg
Sweden
Telephone + 46 (0)31-772 1000

Reproservice
Gothenburg, Sweden 2014

High-Temperature Corrosion Chemistry in Oxy-Fuel Combustion

THOMAS EKVALL
Division of Energy Technology
Department of Energy and Environment
Chalmers University of Technology

Abstract

Drastic cuts in global CO_2 emissions are needed to mitigate the global warming if limiting global warming to 2ºC. The power generation sector is largely based on fossil fuels and produces a significant share of the global CO_2 emissions. Thus, new power generation processes with drastically reduced CO_2 emissions need to be employed to mitigate global warming. Two alternatives which may be part of the solution is the replacement of coal with biomass or to apply the concept of carbon capture and storage (CCS). In CCS the CO_2 is captured and processed on site and thereafter transported to a storage location. Oxy-fuel combustion, which has been studied in this thesis, has been demonstrated in large-scale pilot plants (30-60 MW). This work investigates the possibilities to co-combust biomass and coal in oxy-fuel combustion for CO_2 capture. Biomass combined with CO_2 capture has the potential to contribute to negative CO_2 emissions. However, the high temperature corrosion (HTC) and the related K-Cl-S chemistry need to be studied in detail in order to determine the potential consequences for corrosion on heat transfer surfaces. This, since the use of biomass in power generation is problematic due to the relative high content of alkali (mainly potassium) and chlorine. Together these compounds form KCl, a salt which causes corrosive deposits and subsequent problems with so called high temperature corrosion (HTC). When sulphur is present, alkali sulphates may form instead of alkali chlorides. Sulphates have a higher melting point and causes less problems with corrosion and sulphates are therefore preferred instead of chlorides.

The work in this thesis is based on experiments performed in a 100 kW combustion unit and modelling of chemical kinetics. Both the experimental and modelling results show that a high SO_X concentration is preferable to achieve as high degree of sulphation of the alkali chlorides. In oxy-fuel combustion, the SO_X concentration is typically high due to flue gas recycling, which enables almost complete potassium sulphation in some of the studied oxy-combustion atmospheres. This makes oxy-fuel combustion an attractive process for co-combustion of coal and biomass, since alkali chloride formation to large extent may be suppressed. In addition, the effect of KCl on the CO oxidation process has been studied in air-fuel and oxy-fuel environments. The results show that KCl can promote CO-oxidation in a CO_2 rich environment. However, no change could be observed for the total burnout time even though the CO concentration was decreased.

Keywords: *alkali, CO-oxidation, combustion, experiments, modelling, oxy-fuel, sulphation*

List of publications

This thesis includes the work presented in the following papers

Paper I Ekvall, T.; Normann, F.; Andersson, K.; Johnsson, F., Modeling the alkali sulfation chemistry of biomass and coal co-firing in oxy-fuel atmospheres. Energy and Fuels 2014, 28 (5), 3486-3494.

Paper II Ekvall, T.; Andersson, K.; Johnsson, F., CO-KCl-SO_2 interactions in an 80 kW propane-fired flame - An experimental study comparing air and oxy-fuel combustion To be published in the proceedings of the *Impacts of Fuel Quality on Power production* conference, October 26-31, 2014, Snowbird, Utah

Thomas Ekvall is the main author and responsible for the modelling and experimental work presented in both papers. Dr. Fredrik Normann has contributed with guidance in the modelling together with discussions and editing of the first paper. Associate Professor Klas Andersson has contributed with guidance in the experimental work in the second paper as well as with discussion and editing of both papers. Professor Filip Johnsson has also provided with discussions and editing of both papers.

Acknowledgement

I would like to start to thank my supervisors Assoc. Prof. Klas Andersson and Ph.D. Fredrik Normann for their guidance. Your door is always open and you bring joy to the work also when I have been struggling. I am also thankful for all the help I have got from my examiner Prof. Filip Johnson. Despite the busy agenda there has always been room for discussion. I would also like to show my appreciation to the Swedish Research Council (621-2011-4699) for supporting this project financially.

Johannes Öhlin, Rustan Marberg and Jessica Bohwalli are greatly acknowledged for their help before, during and after experiments has been performed. For learning me everything I know about the oxy-fuel rig and supporting me during several experimental campaigns both Daniel Bäckström and Daniel Fleig are also greatly acknowledged. Dan Gall together with his co-workers is acknowledged for their contribution with both equipment and expertise regarding aerosol measurements. A special thanks to Daniel Bäckström with whom I spend most of my time in Kraftcentralen. It has been a pleasure and your help has been invaluable. Your experimental enthusiasm is spread around you like soot radiation from a propane flame running with only secondary air.

Stefanía Ósk Garðarsdóttir, thank you for sharing your office with me. I appreciate your support and all the help you have provided. Your unfailingly cheerful mood makes it impossible to not enjoy the time at the office. I would also like to thank everyone at Energy Technology for contributing to pleasant working place.

I would like to thank my friends and family for their support. Especially my mother, who has done a tremendous job over the years supporting everything I have been doing. Without all your effort I would most certainly not be writing this thesis. Special thanks also to my father for letting me, already in early years, "help you" when you were fixing things at home. It has taught me how to solve practical problems, awakening my technical interest and truly inspired me to not be afraid of the unknown and to seek for answers.

To my fiancée My: You have given me your full support since day one. This despite that you have been forced to listen to all my stories about experiments that has went well but probably more often about experiments not turning out that well. Together with our son, Rasmus, you have given me inspiration and perspective when I need it the most. For everything you both are I love you truly.

Last but not least I would also like to thank my mother and aunt for letting me borrow their cottage, giving me the opportunity to sit on this porch were most of this thesis has been written.

Thomas Ekvall
Skörbo – Orust - Sweden
August, 2014

Table of content

1 Introduction

Today it is widely accepted that the global temperature increase is a result of anthropogenic use of fossil fuels [1]. As a consequence the interest in alternative energy sources, including biomass and waste based fuels has increased. However, fossil fuels remains the major primary energy resource in heat and power generation world-wide. According to IEA, in 2010 over 65% of the global electricity production was based on combustion of fossil fuels; over 40 % was from coal [2]. There is, thus, a long way to go to replace the present use of fossil fuels.

An alternative path to replacing the fossil fuels is to lower the emissions of CO_2 from the use of fossil fuels by employing the concept of carbon capture and storage (CCS). CCS allows for a continued use of fossil fuels without emissions of carbon dioxide (CO_2). There are four main capturing concepts discussed: pre-combustion for which the carbon is removed before combustion via gasification, post combustion where the CO_2 is separated from the flue gases via e.g. absorption [3], oxy-fuel combustion [4] where the fuel is combusted in a oxygen-flue gas mix instead of air, and chemical-looping combustion where the fuel is oxidized by a metal oxide instead of air [5]. A schematic of each concept is shown in Figure 1. The captured or separated CO_2 is stored underground at a suitable location, such as aquifers or in depleted oil fields [6]. Before transportation to storage the CO_2 stream is cleaned from impurities, such as water, particulates, NO_x and SO_x. Employment of CCS will typically lower the emission of greenhouse gases from fossil fuels with 90-95%. This does however come with a considerable additional cost, specific for each concept.

An interesting possibility to reduce global warming is to combine combustion of biofuels and CCS, which commonly is referred to as “bioenergy with carbon capture and storage” (BECCS). BECCS has the possibility not only to help to reach a zero emission target for power or industrial plants but also to achieve negative emissions. BECCS could be used to compensate for fossil CO_2 emissions from sources where a reduction might be more difficult to achieve. BECCS has also been suggested to be used for actual removal of CO_2 from the atmosphere. Azar et. al [7] has shown it possible to reach the 2°-target even if we, for a while, exceed the required CO_2 level in the atmosphere provided the use of BECCS.

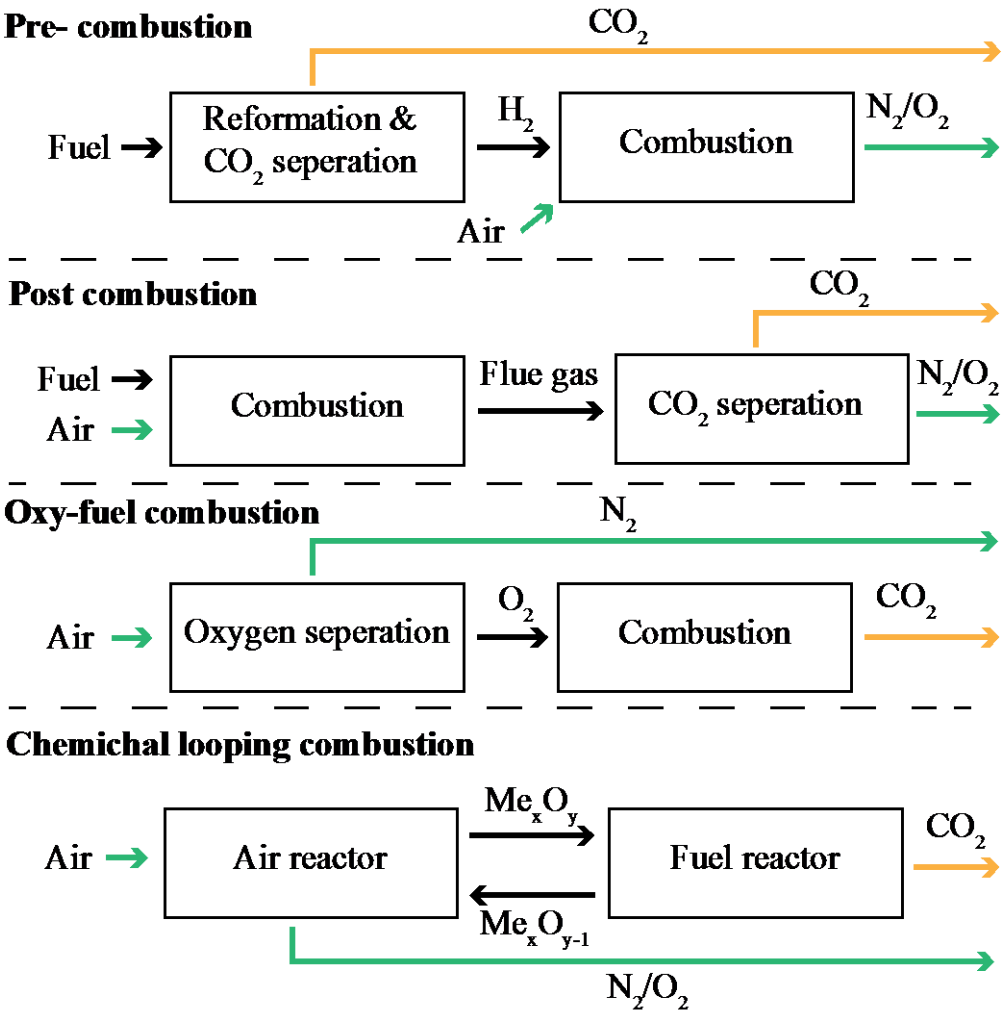

Figure 1. The schematics over the four main concepts for CO_2 separation for heat and power production. In the drawing only the main components (on a dry basis) of each stream are indicated the CO_2 streams might also contain for example NO_X and SO_X that has to be removed before transportation and storage.

1.1 Objective

The presented thesis investigates the combustion chemistry relevant to oxy-fuel combustion of biomass and coal, which is a BECCS technology. In relation to coal, biomass contains relatively high levels of alkali metals (mainly potassium) and chlorine, but on the other hand relatively low levels of sulphur. As a result of the fuel composition significant amounts of alkali chlorides may form during combustion of biomass, which increases the risk for problems with high-temperature corrosion (HTC). However, during co-combustion of coal and biomass the fuel-bound sulphur in the coal may promote sulphation over chlorination of the alkali metals. The HTC related chemistry is investigated in the present work during both in-flame and post-flame conditions. The main focus of the investigation is on the homogenous gas-phase chemistry and includes experimental work as well as combustion simulations. The work has included the development and evaluation of a new methodology with the purpose of investigating alkali chemistry in technical scale combustion test units. The results obtained is used to discuss the following questions:

- How is the combustion process influenced by the presence of alkali and sulphur?
- Which are the key parameters to control the sulphation of alkali chlorides?
- Are there any differences in the alkali-sulphur interactions between air and oxy-fuel combustion?

1.2 Outline of the thesis

This thesis is based on the two included papers together with some additional work which is not yet published. The additional work contains experiments and modelling work which complements the work in Paper I. The overall focus is on the sulphation process. However, the thesis also includes an overview of measurement methods, which can be used in experimental work on alkali sulphation. A short description of the two papers follows below.

Paper I includes modelling work focusing on the homogenous sulphation of potassium chloride. The modelling includes a comparison between co-combustion during air and oxy-fuel combustion together with an evaluation of the related chemistry and the most important parameters.

Paper II focuses on the influence of potassium, chlorine and sulphur on the CO oxidation in the flame zone. The work includes both experiments and kinetic modelling for conditions relevant for both air and oxy-fuel combustion.

2 Biomass and oxy-fuel combustion

This chapter presents the concept of oxy-fuel combustion and describes how it differs from conventional air-fuel combustion. In addition, the characteristics of biomass as a fuel will be presented together with the potential effects of introducing biomass in either an air-fuel or oxy-fuel combustion system.

The present study focuses on two subcategories of biomass: forest- and agriculture-derived biomass. These two types are commonly used as fuel for heat and power generation purposes (see Figure 2 for three types of biomasses). The properties of these biomass types may differ substantially in relation to coal. For example, the moisture content is typically higher which is also the case for alkali metals (sodium and potassium) as well as for chlorine [8-11]. The fuel composition does not only differ between different biomass types, but also is also related to the pre-treatment of the biomass before it is fed to the combustion process, e.g. wood chips, saw dust or torrefied wood, where the latter process tend to alter the amount of sulphur and chlorine content [12]. In the present work, the most common types of biomass are considered, *i.e.* forest or agricultural biomass which has not been pre-treated in thermal processes or similar. The simulated content of alkali and chlorine, in both the experiments and the modelling of this work, is hence significant. This is also typically the case when biomass is used in todays' heat and power generation plants.

Figure 2. Heat and power can be produced from various kinds of biomass, some examples are presented here. From left to right, a) wood logs, b) wood chips (not related to the logs in a) and c) rise husk.

2.1 Oxy-fuel combustion

In oxy-fuel combustion the fuel is combusted in an almost nitrogen free atmosphere obtained by mixing pure oxygen with recycled flue gases. The nitrogen is therefore mainly replaced by CO_2 or a mix of CO_2 and H_2O for dry or wet flue gas recirculation respectively. The concept of oxy-fuel combustion and differences between dry and wet flue gas recirculation is described in Figure 3. The figure also shows examples of components to demonstrate differences between streams. The difference in gas composition in relation to air combustion is then affecting physical properties such as the specific heat capacity and emissivity of the gases resulting in a different temperature profile compared to air firing [13-15]. In order to compensate for such differences, the concentration of oxygen in the oxidizer is most often higher than 21% [4].

The amount of recirculated flue gas is directly related to the feed gas oxygen concentration; a higher concentration requires a lower amount of recirculated flue gas. Also the minor species, in addition to CO_2 and H_2O, in the flue gases will be recirculated as well (if they are not separated before recirculation). The recirculation will therefore influence the concentration of these species; the concentration of SO_2 is typically more than three times higher in oxy-fuel combustion compared to air combustion [16, 17]. Although the concentration of substances such as SO_X and NO_X is low, such a relatively large difference can be of importance for the chemical reactions. It is not only the recirculation itself that affects the gas composition in the furnace, the recirculated composition will also change if flue gas cleaning equipment is placed in the recirculation loop of the system. It is for example likely to separate solids before recirculation and to remove e.g. condensed alkali species (the species indicated in red Figure 3). Another component that can be used is a flue gas condenser. Using a flue gas condenser will remove water (referred to as dry recirculation) and soluble compounds such as HCl and SO_3/H_2SO_4 (the species indicated in blue Figure 3). In this way flue gas cleaning equipment can be used as a measure to achieve a favourable combustion atmosphere. On the other hand, if a cleaning device is put before the recirculation the cost for that specific component will increase due to a larger gas flow compared to a cleaning position outside the loop [4].

In this work, when referring to an oxy-fuel system, it will be similar to the one presented in Figure 3. The system will therefore always include ash removal before the flue gas recirculation and has the possibility to choose whether the flue gas condenser should be used or not. If a flue gas condenser is used before the recirculation it will be referred to as “dry flue gas recirculation” and, if not, it will be referred to as “wet flue gas recirculation”.

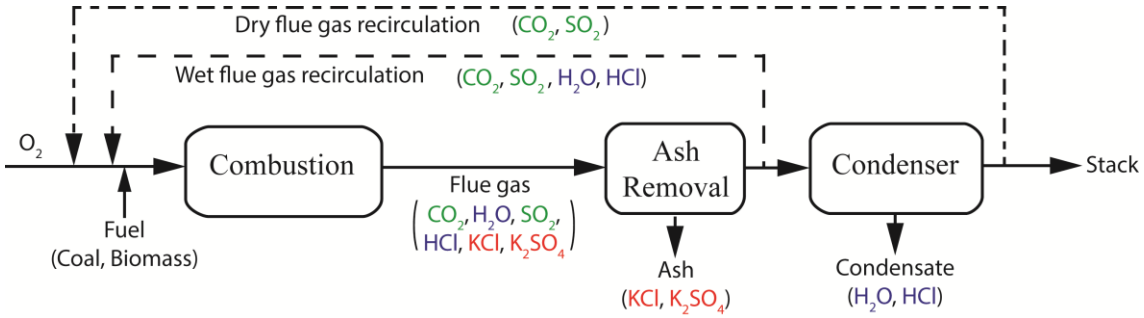

Figure 3. Overview of the oxy-fuel combustion process, indicating potential compositional differences using solids separation and a flue gas condenser. The species indicated in parentheses are examples to clarify differences between the streams. Red indicates solids, blue condensable species and green gaseous species.

2.2 Co-combustion

Co-combustion is a way to introduce biofuels to fossil-fuel fired units in order to achieve a reduction in CO_2 emissions with a fossil origin instead. Biofuels may be co-combusted with coal directly or indirectly. During indirect co-combustion the two fuels are combusted separately and the systems are connected on either the steam or the flue gas side. In direct co-combustion system, on the other hand, the fuels are combusted in the same furnace, with the fuels mixed and fed together, either to a bed (fixed or fluidized) or to a burner with suspension-based combustion [18].

For existing suspension-fired units in which biomass should be introduced for co-firing purposes, the fuel mills typically set the technical limitation for the share of biomass that may be blended into the fuel mix, as discussed by e.g. Savolainen [19]. Savolainen tried to mix coal and saw dust (in a 315 MW_{fuel} boiler) and for high fractions of saw dust (>30%$_{vol}$) the drying capacity of the mills was insufficient. When the share on a volume basis was >50% the boiler capacity was reduced by 25%. However, not only the drying capacity was affected. The fraction of coarse coal particles increased with the share of biomass in the mills [19]. The energy required (both thermal and mechanical) to

prepare the biomass varied with both size and the concept chosen but also with moisture content, where the higher moisture content required more energy [20]. A second option to introduce biomass to a PC boiler is to treat the biomass separately. This option requires an extra biomass mill/crusher and a specialized biomass burner. The new burner can be constructed either to be fired with pure biomass or a blend of coal and biomass [19]. Co-firing biomass with coal may affect emissions such as NO_x and SO_X as well as other properties such as ignition delay [19, 20]. The size and share of biomass particles may also have an either positive or negative effect on the outlet CO concentration, i.e. the burnout conditions [20].

2.3 High temperature corrosion

High temperature corrosion (HTC) is a problem which influences the heat transfer surfaces in a boiler. HTC is caused mainly by metallic salts with a high melting point that favours deposition. Compounds containing alkali metals and chlorine are among the most aggressive, why HTC is primarily a problem for power plants fired with biomass rather than coal [21-23]. To alleviate HTC related problems in biomass fired power plants the steam temperature in the boiler is often lowered with a decreased electrical efficiency as a consequence [8]. The risk for alkali-related HTC might be reduced during co-combustion of coal and biomass (in relation to combustion of pure biomass) due to the relatively high levels of fuel bound sulphur in coal which favours the formation of the less corrosive sulphates over chlorides [9, 24, 25]. Oxy-fuel derived flue gases has been shown by Syed et al. [26] to be more corrosive compared to those derived from air combustion. However, they assumed the level of deposition and composition of the deposits to be the same for both air and oxy-fuel flue gases which is not necessarily the case, a fact which will be discussed further in this work.

2.4 Co-combustion and flue gas recirculation

As mentioned, the flue gas recirculation applied in oxy-fuel combustion increases both SO_X and NO_X concentrations compared to air-fuel combustion [27, 28]. In this work the SO_X components have been studied in detail, components whose concentration level typically is 3-4 times higher in oxy-fuel compared to air-fuel flue gases [17, 27]. An increased SO_X concentration will also increase the S/K-ratio found in the flue gases if the ash (containing the potassium) is removed before the flue gas recirculation. The theoretical relation between S/K in the fuel and the flue gases is shown in Figure 4. The calculations are theoretic and are based on the assumptions that all fuel bound sulphur and alkali species are being released to the gas phase, but also that the formed alkali gas phase species are captured in the condenser water and/or extracted as solids before the flue gas is recirculation to the burner (see Figure 3). The ratio between S/K in the flue gas and in the fuel is one in air combustion but about five in the OF25 dry case (oxy-fuel operation with dry flue gas recycling and with 25 vol.% oxygen in the feed gas). The amount of sulphur in the flue gases is then decreased for higher oxygen concentrations and for wet recirculation in relation to dry. To summarize, the S/K-ratio in the flue gases will always be higher during oxy-fuel combustion if the recirculated flue gas contains sulphuric species. If no sulphur is recirculated it will be a one to one relationship similar to combustion in air. SO_2 is shown to inhibit the oxidation of CO during both air and oxy-fuel combustion hence influencing the overall combustion process [29, 30]. In addition, a high concentration of SO_2 seems to favour sulphation of alkali metals [9, 31, 32].The SO_2 concentration is therefore important for both in-flame and post-flame conditions. It also implies a possible performance difference between air and oxy-fuel combustion due to the possible increase in SO_2 concentration for the latter case.

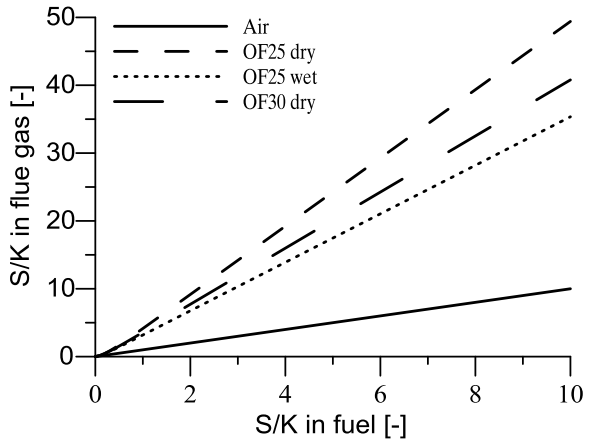

Figure 4. Molar sulphur to potassium (S/K) ratio in the flue gases and how it varies with respect to S/K ratio in the fuel. The theoretical variations are shown for air combustion and oxy-fuel (OF) combustion. There are three cases representing different oxygen concentrations (25% and 30%) and recirculation strategy (wet or dry). In air, the S/K ratio of the flue gas is the same as that of the fuel. The trends are based on the assumption that all sulphur and potassium containing species are released to the gas phase. Source: Paper I.

3 Method

The work is based on two main methodologies: combustion experiments in a 100 kW unit and combustion modelling. The experimental work investigates the chemistry in a technical scale combustor and includes the development of an experimental set up including measurement systems for the analysis of gas and particle composition data (some of the gas phase results are presented in Paper II). The experimental setup is designed to isolate the chemistry of interest. The experimental results are evaluated by means of a reaction model which is based on input data from the experiments. The modelling part also includes a detailed evaluation of the homogenous gas-phase chemistry (Paper I). In this section all included methods will be described in further detail.

3.1 Measurement techniques

Several measurement techniques have been used in this work for characterization the behaviour of alkali sulphation together with the interaction between K, Cl and S on the CO oxidation. In general, the gas composition measurements were conducted by means of standard on-line gas analysis instruments. However, the SO_3 measurements together with the particle extraction and characterization measurements were performed using systems which are not typically considered as standard systems in combination with flame measurements. The principles of the SO_3 and particle measurement systems are therefore also included in this section.

3.1.1 Gas composition

Gas composition measurements are carried out using a suction probe, which samples gas from the furnace. The sampled gas is transported to the analysing equipment by using a heated sampling line. Standard gas analysers (Rosemont NGA 200) were used for CO, CO_2, O_2 and SO_2. The instruments use the paramagnetic principle (O_2), non-dispersive ultraviolet sensors (SO_2) and non-dispersive infrared sensors (CO and CO_2). HCl and SO_3, on the other hand, were measured using FTIR (Bomem MB9100) and by means of controlled condensation, respectively.

3.1.1.1 Controlled condensation

Controlled condensation is a measurement technique for measuring SO_3 (as H_2SO_4) in flue gases. It has been reported to have a similar or better accuracy compared to the "salt method" and isopropanol absorption under both air and oxy-fuel conditions [33, 34]. Thus, this method was chosen for this work. The flue gas sample is cooled down in a water bath to a temperature between 80°C and 90°C, see Figure 5. For the concentrations found in flue gases, this temperature interval is located between the dew point of sulphuric acid (H_2SO_4) and water vapour. In the presence of water vapour SO_3 will form sulphuric acid, which will condense in the cooling tube, while the water vapour follows the main gas stream. The condensed acid is collected during a defined time period (lower concentration requires longer measurement time) with a defined volume flow. The collected acid is quantified by titration in order to determine the amount of sulphuric acid from which the concentration of SO_3 in the flue gases is calculated. It is important to keep the flue gas temperature above the dew point of sulphuric acid before the temperature controlled condenser to avoid sampling losses. In this work an oil heated probe was used to sample the flue gas.

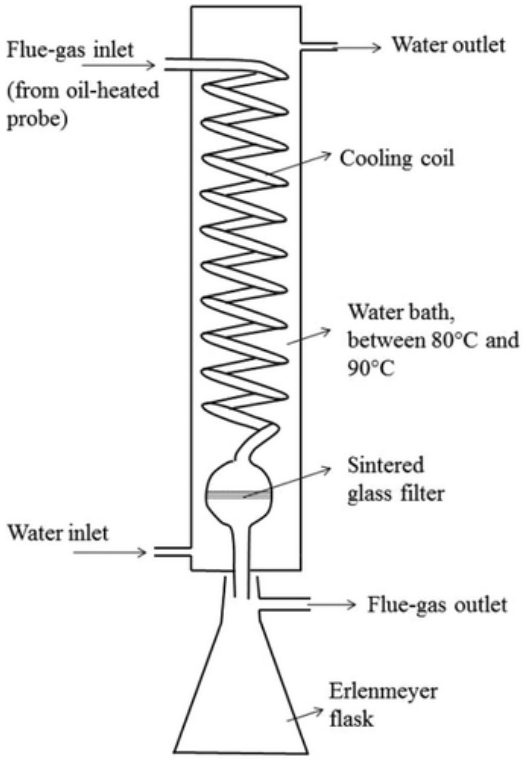

Figure 5. A schematic of the cooler used for SO_3 measurements in this work.

3.1.2 Particle measurements

Most combustion processes form particulates such as soot and inorganic aerosols. Measurements of such particulates at flue gas temperatures below 500℃ have been performed and presented in literature for several different fuels and combustion technologies. In such measurements, different types of suction probes have been used [35-41]. These types of suction probes basically consist of a temperature-controlled tube with an inner tube through which the flue gases may be isokinetically sampled from the furnace. The probe is cooled using a cooling media and the sample gas is also cooled by a dilution gas injected into the probe tip. The extracted particles are then quantified and analysed using suitable measurement techniques as described below.

3.1.2.1 Extraction of particles

Extracting particles at high temperatures (above 600℃) is difficult, especially during biomass combustion when the concentrations of inorganic species (which typically condenses at such temperatures) are relatively high. Condensation might affect the result by changing both the composition and size of the particles during the extraction. Valmari et. al [42] avoided condensation by inserting their equipment into the flue gas path (convection path, about 650℃). Strand et al. [43] and Lind et al. [44] have performed high temperature (750℃ and 830℃ respectively) particle extractions using a suction probe designed to meet the criteria required regarding cooling rate, dilution and residence time in order to avoid problems with agglomeration and/or condensation of gaseous compounds. Wiinikka et al. [45] have presented results from particle extractions from a 8 kW wood pellet combustor for even higher temperatures, up to 1450℃, which corresponds to in-flame temperature conditions. Similar experimental setups have been used also more recently, e.g. by Fernandes et. al [46] even though they measured at lower temperature around 900°C.

The extracted sample should be diluted with a high dilution ratio (1:100) so that the vapour may condensate on the probe walls instead of on the already existing particles, thus minimizing the risk of an altered particle size distribution [43]. It is also important to have a cooling rate above 600℃/s

favouring homogenous nucleation over heterogeneous nucleation. This will produce many nano-sized small particles but keeps the sampled particles more unaffected [47, 48]. Coagulation of particles can take place spontaneously due to relative motion and is strongly dependent on particle concentration and residence time. A residence time of 0.2 s is sufficient for a particle concentration of 10^{18} to decrease with as much as a factor 1000. This will increase the mean particle diameter correspondingly [49]. A high dilution rate and a short residence time between the probe tip and the measurement equipment is therefore to prefer. For the particle measurements performed in this work the gas temperature at the probe inlet is lower than 250°C, which enables a sufficient cooling rate. The dilution rate in the probe (of about five) results in a residence time in the probe of about 0.5 s, which is too short for any significant wall condensation to occur. Furthermore, the probe temperature is kept at 120°C. The probe is connected to a vacuum pump which draws the sample gas from the tip of the probe.

3.1.2.2 DLPI

The mass size classification of particles is usually done by using a low-pressure impactor (LPI) which separates particles in the range of 30 nm – 10 μm. A cascade impactor has the lower limit at 300 nm, see Figure 6 for a principle drawing of an impactor. Cyclones are used for collecting larger particles, and for preventing large particles to fill the top stage in the LPI [35-41, 47, 48, 50]. Today the most common LPI is the Dekati low pressure impactor (DLPI). The DLPI has a slightly different design and two additional stages (13 in total) giving a better performance compared to the older generation, the so called Berner low pressure impactor (BLPI) [50].

The performance of a LPI is related to temperature and pressure conditions. For a BLPI an increase in temperature from 20℃ to 160℃ changes the cut diameter (also referred to as d_{50} which is the particle size collected with a 50 % efficiency) with 5 to 50%; the highest deviation is found for the smallest particles [42]. It is therefore important to consider the LPI calibration conditions. Performance parameters for other temperatures than the calibration temperature may be estimated by correlations [42, 51]. In this work the DLPI has been heated up to 100°C, which is higher than the calibrated temperature, in order to avoid condensation of flue gas species within the DLPI.

On each of the LPI stages there is a collector. The collectors usually consist of a piece of aluminium foil coated with vacuum grease to prevent the particles from moving on the foil. If the LPI is operating at high temperatures, other materials are used for the collectors. The collectors should be heated up both before and after operation in order to dry the samples and to minimize the weighing error due to humidity [35, 37, 42, 44].

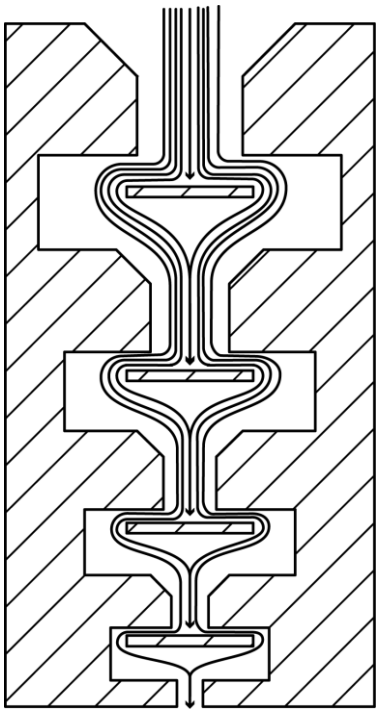

Figure 6. Simplified drawing of an impactor for measurements of gravimetric particle size distribution. The sample stream enters at the top into the first collection plate. The largest particles hit the plate while the smaller tend to follow the gas stream to the next stage. Each stage is smaller than the previous which increases the flow speed and forces also smaller particles to hit a collection plate.

3.1.2.3 SMPS and VTDMA

The scanning mobility particle sizer (SMPS) is a system widely used for atmospheric particle measurements but also for measurements in combustion processes [37, 39, 41, 43, 52]. An SMPS consists of two parts: a differential mobility analyser (DMA) and a condensation particle counter (CPC), both described in Figure 7. The DMA technology has been used for a long time to characterize aerosols in gas flows [53]. The DMA uses two coaxial cylinder electrodes to create an electrical field perpendicular to the sample stream. The electrodes are usually two coaxial cylinders avoiding the end effects following with the use of plates [54]. There is a relation between electrical field and the particle velocity and diameter which makes it possible to control the size of the particles exiting the instrument. The particles are charged before entering the electrical field. In the SMPS system used in this work the particles are charged via bipolar diffusion created by a radioactive source (^{85}Kr). As shown in Figure 7 (left part) the charged particles enter a laminar flow of inert gas, typically N_2. Due to the laminar flow conditions applied, the horizontal motion of the particles is in principle influenced by the electrical force between the particles and the charged cylinder in the middle of the chamber. The horizontal velocity will be higher for smaller particles (blue in the figure) and will therefore reach the centre before they reach the openings in the centre cylinder. The opposite will occur for particles which are too large (red in the figure), which will not reach the centre or will do so first below the openings. By controlling the vertical velocity and the electrical field (the horizontal velocity) it is possible to decide the diameter of the particles leaving the DMA (green in the figure). Even though there are systems developed for detection of particles down to 1 nm the DMA is most commonly used for detection of particles between 10 nm and 1000 nm. For particle diameters smaller than 10 nm the risk for particle losses due to Brownian diffusion is increased, which then would cause problems already upstream the DMA [54-56].

The monodisperse particle flow exiting the DMA is introduced to the CPC that measures the number of particles passing by the detector (right hand part of Figure 7). In this way the SMPS measures the particle number for a certain size of particulates. In the CPC the particles are coated with a liquid (in this work it is iso-butanol) increasing the particle diameter before entering the detection chamber. The detection chamber consists of a light source and an optical detector by means of which the particles can be counted.

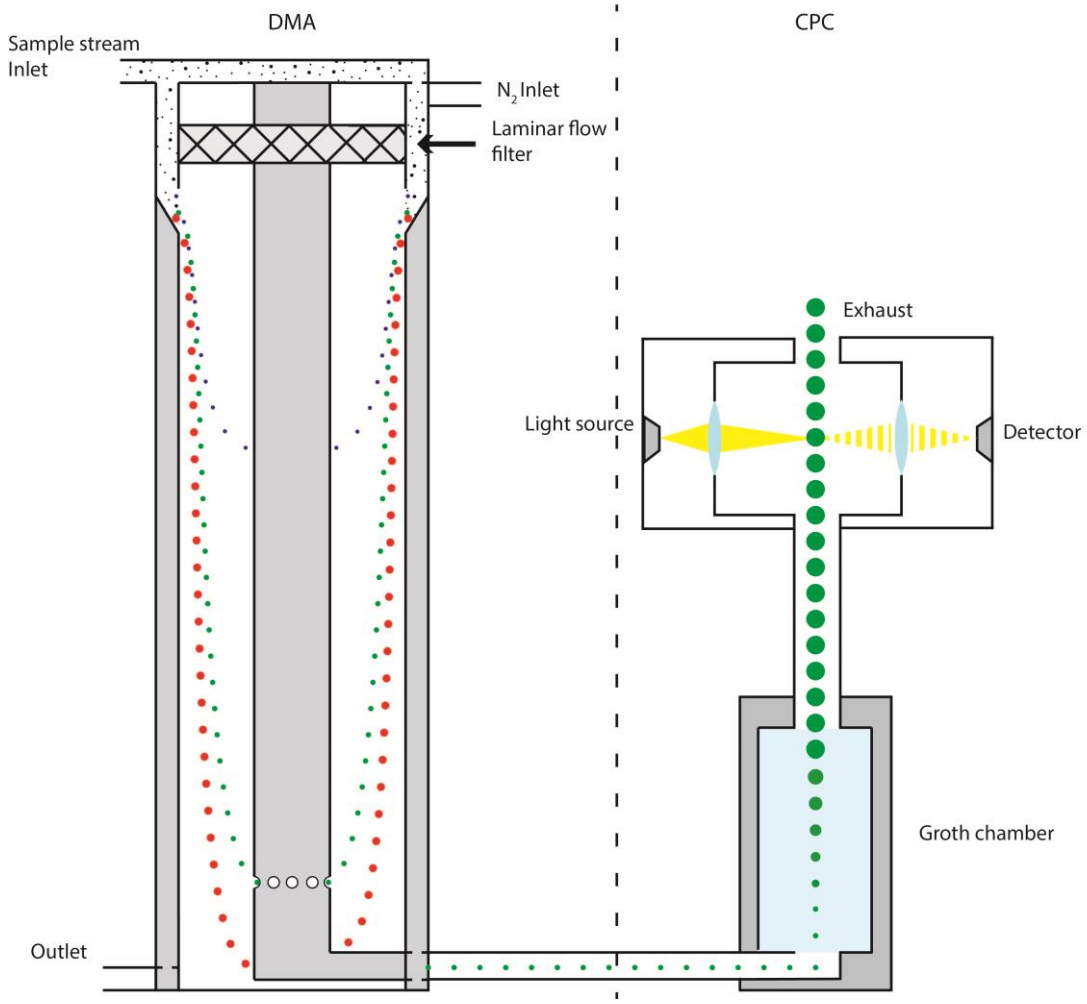

Figure 7. Functional description of a SMPS consisting of two parts, a DMA (to the left) and a CPC (to the right) connected in series.

A volatility tandem DMA (VTDAM) is obtained by adding a second DMA together with an oven prior to the SMPS. The VTDMA is used to quantify the volatility of the particles [55]. A monodisperse particle flow is created by the first DMA which are heated in the oven before entering the SMPS. It is now possible to estimate the degree of devolatilisation by measuring the change in particle size distribution.

3.2 Combustion experiments

In this work, experiments were performed in the Chalmers 100 kW test unit as presented in Figure 8. The unit may be operated in air- or oxy-fuel mode. The furnace is 800 mm in diameter and has a height of 2400 mm with a propane burner mounted at the top of the furnace. There are four water-cooled rods for temperature control inside the furnace. The furnace has measurement ports at seven distances from the burner (M1-M7) and there are eight measuring ports (M8-M15) further downstream in the flue gas path. The burner is fed with 1.73 g/s of propane and oxidizer corresponding to a

stoichiometric ratio of 1.15. The experimental unit facilitates SO_2 injection direct into the oxidizer before entering the primary and secondary register. As a part of this work a KCl injection system has been developed to investigate the alkali chemistry during combustion experiments. The KCl is fed as an aqueous solution via a probe through the furnace ceiling (see Figure 8). At the tip of the probe a nozzle is spraying the solution directly into the flame 40 mm downstream of the burner. The KCl-water solution is kept at a salt-concentration of 3.4 wt.%. The solution is stored in a separate tank with an internal circulation pump to avoid salt precipitation. A metering pump is used to inject 0.9 l/h of the KCl(aq) solution into the flame. The KCl(aq) injection system is shown in Figure 9.

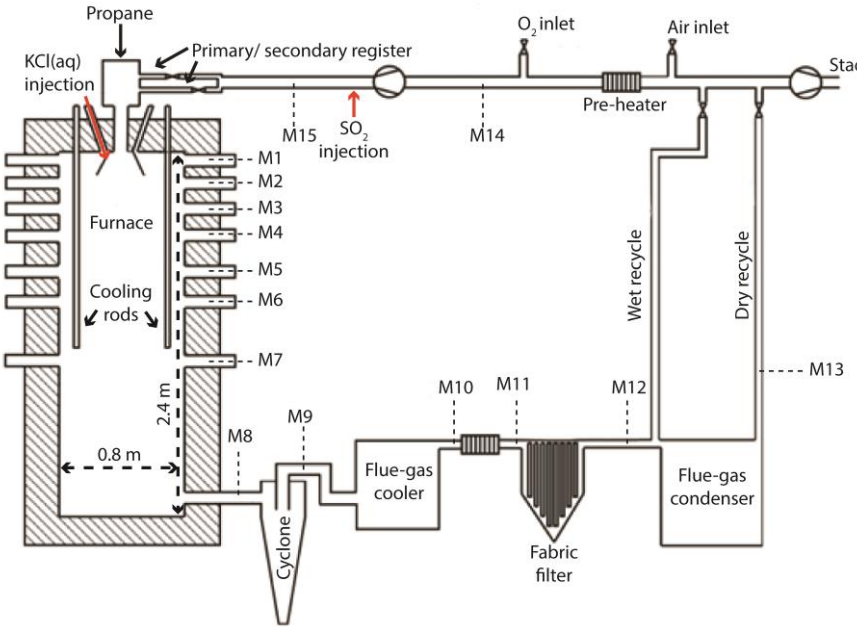

Figure 8. Schematic drawing of the 100 kW test unit at Chalmers University of Technology. Red arrows indicate the position for injection of KCl and SO_2. The locations of the 15 measuring ports are indicated as M1-M15.

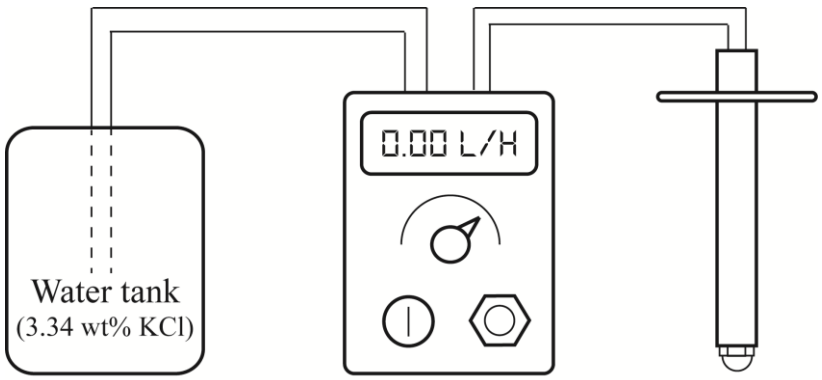

Figure 9. A schematic drawing of the salt injection setup including storage tank, metering pump and injection probe.

The injection of KCl(aq) is constant and the S/K-ratio is altered by changing the amount of SO_2 injected. The amount of SO_2 is controlled by adjusting the concentration in the oxidizer. During operation with flue gas recycle, SO_2 is recycled to the burner inlet. Some sulphur is, however, lost in the flue gas system, due to absorption in condensing water and reactions with deposits in filters etc. The loss of sulphur in the loop varies with time, but the SO_2 concentration in the oxy-fuel oxidizer is kept constant for each case by controlling the injection of SO_2. Table 1 presents the conditions for which the degree of sulphation is investigated. The SO_2 concentration has been measured to decrease with 11% from M8 to M13. The sulphur concentration in each oxy-fuel case is based on this drop in

SO_2 concentration of 11 % in the recirculation loop. A sulphur to potassium ratio of 4 (S/K=4) was used for both the sulphation experiments (Paper I) and the CO experiments (Paper II) with the exception that the injection of KCl and SO_2 were tested individually and in addition injection of pure water was used for CO measurements.

Table 1. Running conditions of the experimental cases.

	Fuel feed [g/s]	**O_2/fuel ratio [-]**	**O_2 oxidizer [% wet]**	**O_2 stack [% wet]**
Air	1.73	1.15	21	2.55
OF25	1.73	1.15	25	3.00
S/K (injected)	**KCl(aq) [l/h]**	**SO_2 injection* [g/h]**	**SO_2 oxidant [% wet]** **Air**	**OF25**
1	0.9	26.5	94	418
2	0.9	53.0	189	971
4	0.9	106.0	567	2022
6	0.9	159.0	756	3068
8	0.9	212.0	1323	-

**Varied to keep the inlet concentration constant for the OF25 case*

The flue gas composition is measured along the centre line at M2 to M5, M7 and M8 using a water-cooled suction probe .In addition, the oxidizer composition is measured at M15. As discussed in greater detail in the measurement section, the gas composition (CO, CO_2, O_2 and SO_2) was measured with standard gas analysers while HCl was measured with a FTIR designed for gas composition analysis, and, SO_3 was measured with the controlled condensation method. Particle measurements are performed in the centre position at M3 with an oil-cooled probe. The probe has a dilution ratio of 5 and is connected to a DLPI for particle sampling. A slipstream might also be used for analysis in a SMPS and VT-DMA. This slip stream is further diluted achieving a total dilution factor of about 35.

3.3 Simulations

The simulations of the gas-phase combustion chemistry presented in this work is divided into two parts: flue-gas simulations (Paper I) focusing on reaction paths and operational parameters of importance for the sulphation of KCl, and, combustion simulations including the oxidation of hydrocarbons, alkali sulphation and the interactions between CO and sulphur, potassium and chlorine species (CO-oxidation simulations in Paper II). The simulations are compared with the results obtained from experiments performed in this work. The simulations are performed using the software CHEMKIN PRO. The reactor is modelled as an isothermal reactor, or a reactor with fixed temperature profile, applying plug-flow conditions. A detailed reaction mechanism describes the combustion chemistry. The reaction mechanisms used for the combustion and flue gas simulations and also the sensitivity analysis are described below.

3.3.1 Reaction mechanism

The chemistry relevant for sulphation of potassium during post flame conditions includes the subsets: CO/H_2, S, Cl and K. The subsets used in this work are based on the mechanism presented by Hindiyarti et. al [57]. The complete mechanism has been validated by Hindiyarti et. al [57] against experiments by Iisa et al. [58], Jensen et al. [59] and Jimenez and Ballester [60, 61]. This work also includes an additional subset approximating the condensation of K_2SO_4 as presented by Li et al. [62].

The mechanism by Hindiyarti is derived for post-flame condition and does not include any combustion chemistry. For the simulations which also include the combustion process, three more subsets were added to the mechanism describing the oxidation of C1, C2, and C3 hydrocarbons respectively. The hydrocarbon oxidation subsets are based on the works by Glarborg et. al [63, 64], Alzueta et. al [65] and Abián et. al [66]. All subsets together with the included reactions and their properties are listed in the Appendix.

The combined potassium sulphation and hydrocarbon oxidation mechanism has not been validated, although the included subsets have been validated individually in previous work. Therefore, this work evaluates the influence of the C1-C3 subsets on the sulphation chemistry. An example from the evaluation is presented in Figure 10. Figure 10a shows the mole fraction of K_2SO_4 at the outlet of an isothermal PFR calculated with and without the C1-C3 subsets. There is a noticeable relative difference at temperatures below 700°C, where the sulphation is initiated at slightly lower temperatures. These temperatures are lower than what Ilisa et al. [58] applied in their work, a study which was used by Hindiyarti et al. [57] for validation purposes. Figure 10b and c shows the formation of K_2SO_4 at 660°C and 1000°C respectively. For the lower temperature the sulphation process is faster when the hydrocarbon chemistry is included (although no hydrocarbons are present). At higher temperatures no difference is observed. The degree of sulphation and the equilibrium is not affected by including the C1-C3 subsets. In summary, there may be a small but noticeable effect at temperatures below 700°C by merging the two mechanisms, which deserves attention. In this work the merged mechanism is used to evaluate the experimental work based on an 80 kW propane flame, which is obviously not an ideal set-up for validating the mechanism. However, the combination of the modelling and experimental results strongly indicates that the employed mechanism is appropriate for the purpose of this work.

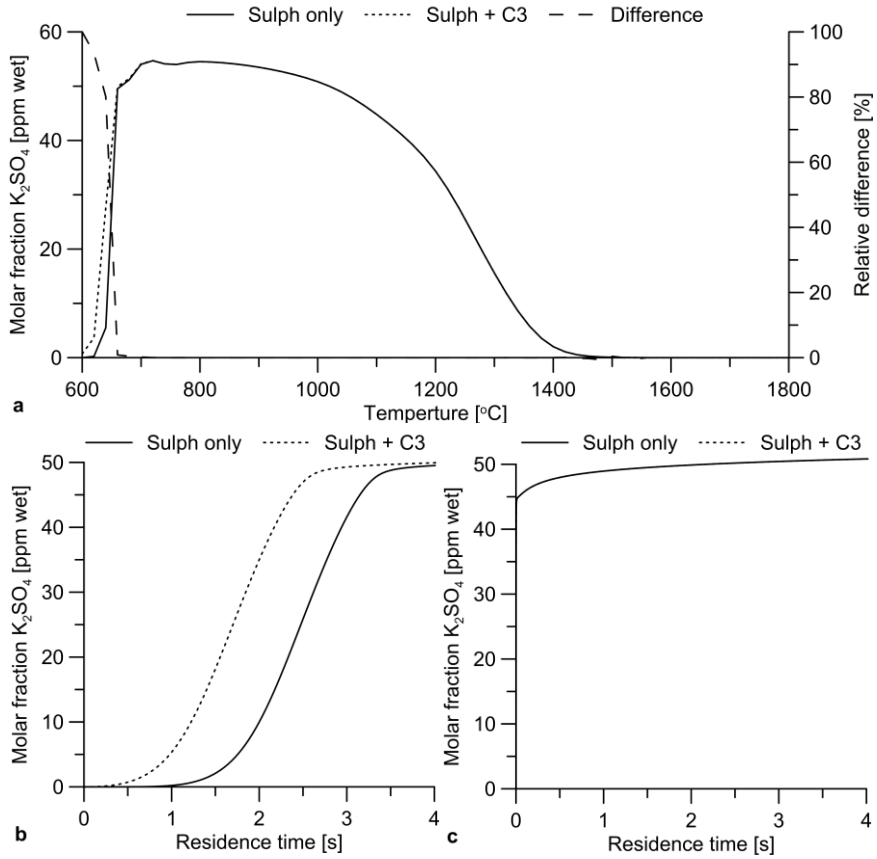

Figure 10. Result from an isothermal PFR model including only the sulphation mechanism and the sulphation mechanism together with the C1-C3 subsets. The PFR is fed with a gas flow with the following composition: 20 % CO_2, 20 % CO, 12.5 % O_2, 400 ppm SO_2, 100 ppm KCl and N_2 set by difference. a) Molar fraction of K_2SO_4 at the outlet for temperatures between 600°C and 1800°C together with the relative difference between the two mechanisms. b) and c) Molar fraction of K_2SO_4 throughout the reactor at a temperature of 660°C and 1000°C respectively.

3.3.2 Combustion simulations

The combustion simulations basically include two cases representing Air and OF25 conditions. In order to keep the modelling and experimental results separated the modelled cases will be denoted as Air_M and $OF25_M$. The model is based on the experimental work. The same reactor geometries and temperature profile (see Figure 11 for the temperature profile) is used in both cases. The reactor residence time is, thus, different between the two cases (4.4 s for the Air_M case and 5.6 s for the $OF25_M$ case) due to the differences in volumetric flows. To describe the influence of the radial mixing in the flame zone (which is assumed perfect in a PFR) the oxidizer is staged as is shown in Figure 11. The same cumulative oxidizer injection profile is used in both cases. The fuel (propane) feed and oxidizer inlet composition is the same as in the test unit during the experiments (see Table 1).

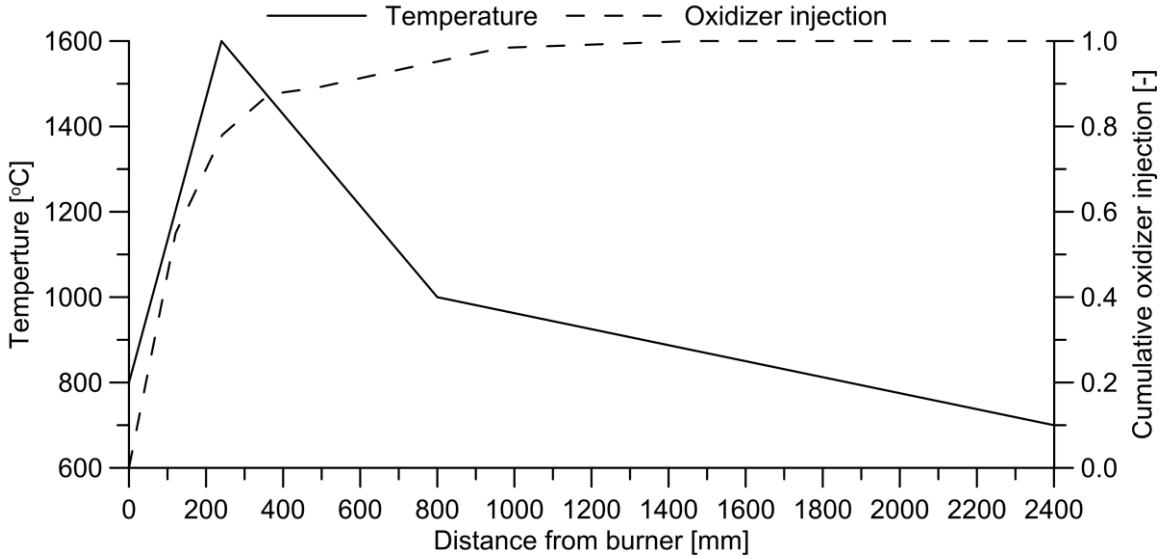

Figure 11. The temperature profile (solid line) and cumulative oxidizer injection profile (dashed line) used for the simulations including combustion of propane.

3.3.3 Flue gas simulations

The flue gas simulations includes an air fired case and two oxy-fuel cases both with 25 % oxygen but applying wet and dry flue gas recirculation denoted Air_{FG}, $OF25_{FG}$ wet and $OF25_{FG}$ dry, respectively. For these cases the temperature profile is linearly decreasing from 1600°C down to 500°C. In all three cases the same reactor geometry is used causing differences in residence time, see Table 2. The inlet composition, presented in Table 2, is based on complete combustion (stoichiometric-ratio equal to 1.2) of a fuel mix of 90% coal and 10% biomass. It is assumed that all S, K and Cl are released to the gas phase. For more details on how the inputs are derived, see Paper I.

Table 2. Inlet mole fractions used for flue gas simulations. The concentrations are presented on a wet basis

	Air_{FG}	**$OF25_{FG}$ dry**	**$OF25_{FG}$ wet**
N_2	73.9%	6800 ppm	4820 ppm
CO_2	14.5%	85.5%	60.7%
H_2O	8.30%	9.75%	34.8%
O_2	3.27%	3.85%	3.85%
SO_2	417 ppm	2245 ppm	1620 ppm
KCl	96 ppm	112 ppm	112 ppm
HCl	6 ppm	7 ppm	287 ppm
Residence time [s]	4.0	4.6	4.6
SO_2/KCl ratio	4.4	20	14

3.3.4 Sensitivity analysis

A sensitivity analysis is performed to evaluate the effect of important process parameters on the sulphation of potassium chloride. The sensitivity analysis includes the effects of temperature, concentration of O_2, SO_2 and HCl, and a combustion atmosphere based on N_2, CO_2 or a mix between CO_2 and H_2O. The reactor settings are shown in Table 3. Furthermore, a sensitivity analysis of the effect of KCl on CO oxidation is performed. The analysis is performed under isothermal and chemically reducing conditions at various temperatures and CO_2 inlet concentrations. The same conditions are then investigated both with and without KCl in the system. The inlet mole fraction and the interval investigated of each component can be found in Table 4. The reactor temperature is varied between 1000°C and 1600°C. For more details regarding the sulphation and CO oxidation sensitivity analyses, see Paper I and Paper II respectively.

Table 3. Reactor setting used for the sulphation sensitivity analysis.

	Atmosphere			Interval analyzed for
	N_2	**CO_2**	**CO_2/H_2O**	**each parameter**
N_2	73.6%	-	-	-
CO_2	10.2%	83.8%	48.7%	-
H_2O	13.6%	13.6%	48.7%	-
O_2	2.55%	2.55%	2.55%	2%–20%
KCl	100 ppm	100 ppm	100 ppm	-
SO_2	100 ppm	100 ppm	100 ppm	0–100ppm
HCl	0	0	0	0–100ppm
Residence time [s]	4	4	4	-
Temperature [°C]	1600–500	1600–500	1600–500	1600–500

Table 4. Inlet mole fractions used for the modelling work. For the species with a given interval the inlet mole fraction is varied for different cases. In all cases the amount of N_2 is set by difference

	N_2	**CO_2**	**KCl**	**H_2O**	**CO**	**O_2**
Inlet mole fraction	b/d	0-0.95 %	0-626 ppm	5.2 %	2150 ppm	75 ppm

3.4 Data evaluation

This section defines the parameters used to evaluate the results. The parameters are based on the data obtained from both experiments and simulations.

The degree of sulphation is defined as the ratio between the amount of potassium bound as sulphates at a certain position and the total amount of potassium entering the system (Equation 1). However, the amount of K_2SO_4 could not be measured and for the experiments the concentration of HCl is used to approximate the degree of sulphation (Equation 2). Equation 2 is based on the assumptions that HCl and KCl are the only chlorine containing species, that KCl and K_2SO_4 are the only potassium containing species, and that the formation of HCl results from the sulphation of KCl. The simulation results show a negligible difference between Equation 1 and Equation 2 at the reactor outlet for cases where KCl is the only chlorine containing inlet specie, which is also the case in all experiments.

$$\frac{2n_{K_2SO_4}}{n_K^{inlet}} = degree\ of\ sulphation \qquad \textbf{Equation 1}$$

$$\frac{n_{K_2SO_4}}{n_{KCl}^{inlet}} \approx degree\ of\ sulphation \qquad \textbf{Equation 2}$$

To analyse the reaction paths the activity of each reaction is calculated. The activity, R (mol/cm^3), for each reaction, i, is calculated according to Equation 3 by integrating the reaction rate, r, over the reactor residence time. In this way the total activity of a reaction throughout the reactor is determined. This is an efficient way to compare the activity of the vast number of reactions, but of course at the expense of losing the time dependence.

$$R_i = \int_{t_0}^{\tau} r_i dt \qquad \textbf{Equation 3}$$

The influence of KCl on CO oxidation rate is estimated by comparing the outlet concentration of CO in systems with and without KCl according to Equation 4. A ratio above unity indicates an inhibiting effect of KCl on CO oxidation and a ratio below unity indicates a promoting effect.

$$\frac{n_{CO}^{KCl}}{n_{CO}} = CO\ outlet\ ratio \qquad \textbf{Equation 4}$$

4 Theory

This chapter describes the release/formation and interaction of gaseous K, Cl and S containing compounds during combustion. In the present work, K represents the overall alkali metal content in flue gases. In a practical combustion system, sodium (Na) is also typically present but potassium is usually the main alkali specie. In addition, sodium has been reported to follow a similar reaction mechanism as potassium [9, 11, 57, 67].

4.1 The release of inorganic species during combustion

SO_2, HCl and KCl are some of the main inorganic components released during combustion and devolatilization. Their relative release is, however, highly dependent on the overall fuel composition and temperature. The inorganic species are released to the gas phase as a result of the increased temperature. Chlorine is released early in the heating process; up to 50 wt.% of the chlorine may be released already at 500°C [68]. Chlorine is released as chlorinated hydrocarbons, HCl or KCl. The chlorinated hydrocarbons often react soon after the release with subsequent formation of HCl during combustion [68-70]. Potassium is mainly released as KCl, if Cl is present, otherwise it is released as atomic potassium (K) or as hydroxide (KOH) [68-71]. The potassium release has been shown to be strongly coupled to the chlorine release [68]. Chlorine species has a higher tendency to react with char than K-species, which indirectly affects the K release since less Cl is available for KCl formation [70]. The release of Cl and K is also affected by the ash composition. Silicates, especially aluminium silicate (during co-combustion of coal and biomass mainly derived from coal), are shown to be the main component responsible for inhibiting the release of alkali chlorides [25, 71-75]. In addition, the state at which the specie is released in, depends on the combustion temperature in relation to the melting and evaporation temperature for each specific compound, and, also the composition of the fuel and the flue gas [68, 70, 71, 73-78].

Sulphur is released to the gas phase in the form of simple reduced species such as CS_2, COS and H_2S [69, 79, 80]. In the presence of oxygen, these compounds form oxides (mainly SO_2), which are more stable also in a reducing environment [69, 79]. The formation of SO_3 is thermodynamically favoured at temperatures lower than 600°C, but kinetics inhibits the SO_2/SO_3–equilibrium to be reached. The homogenous formation of SO_3 from SO_2 is a result of either the reaction,

$$SO_2 + O(+M) \rightleftharpoons SO_3(+M) \qquad \textbf{R 1}$$

at higher temperatures or the combination of the reactions,

$$SO_2 + OH(+M) \rightleftharpoons HOSO_2(+M) \qquad \textbf{R 2}$$
$$HOSO_2 + O_2 \rightleftharpoons SO_3 + HO_2 \qquad \textbf{R 3}$$

during the flue gas cooling process. The homogenous SO_3 formation is well known compared to the possible heterogeneous reactions that may include fuel and ash particulates contributing to the SO_3 formation [69, 79].

4.2 Formation of alkali containing aerosols

Aerosols formed during biomass combustion vary in size distribution and concentration as well as composition depending on fuel composition and combustion conditionsy. A summary of experimental results from particle measurements at different facilities is found in Table 5. The results represent combustion of different biomasses and a variation of combustion conditions in terms of different combustion technologies and thermal load conditions. The sampling temperature also varies, from 100°C (in the work by Wierzbicka et. al [39]) for the lowest temperature up to 850°C (in work by Valmari et. al [38]). However, K, S, Cl and C (excluding eventual oxygen) are the most common components found in particles from combustion, especially among the smaller particles up to 1µm [35-39, 81].

Table 5 Experimental result find in literature showing the variation in composition, size and concentration of aerosols formed during combustion of biofuels.

Authors	Boiler type	Thermal effect [kW]	Fuel	Sampling temperature [°C]	Particle load [mg/Nm^3]	Main size (by mass) [µm]	Main components (by mass)
Wierzbicka et. al [39]	grate	1000-1500	Sawdust pellets, forest residues	100-175	51-120	5	K, S, Cl
Valmari et. al [38]	CFB	35000	Forest residues, willow	810-850	600-1200	~10	Ca,Si,P,K,S,Cl
Pagles et. al [37]	grate	1000-6000	Forest residues	150-215	79-145	1-10	K, S, C
Johansson et. al [36]	Pellets burner	11-22	Wood pellets, wood briquettes	-	34-240	<1	K, S, Cl
Boman et. al [35]	Pellets burner	10-15	Pellets	-	-	~0.3	K, Cl, S, C
Christansen and Livbjerg [81]	-	15000	Straw	120	3-500	~0.3	K, Cl ,S

When gaseous potassium chloride condenses in an inert atmosphere (homogeneous nucleation) the condensed phase will consist of both monomers and dimers. Such a system will always be in equilibrium [82]. The nucleation is a continuous process where more and more aerosols form until the particle concentrations is sufficient to on-set coagulation. According to Jensen et al. [59] the coagulation half time for particle number concentrations is over 10 seconds at a particle concentration of $3x10^7 cm^{-3}$. The system examined by Jensen and co-workers had a residence time below 2 seconds and for this reason the impact of coagulation was omitted in their model. These assumptions together with mathematical expressions describing e.g. size distribution density functions were used by Jensen et al. to describe the homogenous nucleation of potassium chlorides in a plug flow reactor. In their experiments they showed that when SO_2 is introduced to their experimental set up the amount of particles is drastically increased, which also followed from the model results. Potassium which is homogenously sulphated has a vapour pressure several orders of magnitude lower than KCl and therefore the sulphates are super saturated and forms aerosols through homogenous nucleation[59].

Alkali metals may form carbonates instead of sulphates in the flue gas. The carbonisation has been suggested to follow a heterogeneous reaction path, due to the thermodynamic instability of K_2CO_3(g). The potassium carbonate is suggested to be formed via reaction between KOH(s, l) and gaseous CO_2 [83]. Carbonates may only form at temperatures lower than the temperature where the homogenous sulphation may take place [57, 58, 84].

4.3 Alkali sulphation

The chlorinated form of potassium, KCl, is the main potassium compound released to the gas phase. KCl may however be sulphated during combustion. The sulphation is considered complete when all potassium has formed potassium sulphate (K_2SO_4). At temperatures lower than 450°C sulphated potassium may be found as pyrosulphate ($K_2S_2O_7$) [85]. Such low temperatures are however not relevant for this work. The sulphation of potassium chloride is suggested to follow one of two possible paths: homogenous sulphation where the sulphates are formed in the gas phase (and condens after its formation), or heterogeneous sulphation which includes surface reactions of non-gaseous chloride particles. Below follows a short summary of the previous work on these two suggested reaction paths.

4.3.1 Heterogeneous alkali sulphation

The heterogeneous sulphation of KCl is proposed by Steinberg and Schofield [86] as a surface reaction phenomenon taking place under post flame conditions. In their work with hydrogen and propane flames Steinberg and Schofield concluded sodium sulphate to be too unstable during flame conditions to be responsible for the observed sulphation [86-88]. Experimental results presented by others have, on the other hand, suggested the heterogeneous path should to be too slow to describe the sulphation typically occurring in industrial scale boilers [58, 89].

Sengeløv et. al [84] has shown that the sulphation of condensed KCl increases with increasing temperature and oxygen concentration. The amount of water in the surrounding gas does not seem to influence the sulphation. Sengeløv et al. [84] suggest that only small KCl particles (<1µm) can reach a significant level of sulphation at residence times below 1 second even at high temperatures. However, KCl aerosols in this size are unlikely to be found at temperatures above 800°C and at lower temperatures the sulphation of condensed KCl is less than 20% [62, 84]. These modelling results are in agreement with experimental results that can be found in literature [58, 62, 89]. This work focuses on the homogenous alkali sulphating route, which is more relevant for the conditions studied here which are represented by flame temperatures up to about 1600°C. However, it should be noted, that the findings presented are valid for residence times in the range of seconds. Once deposited, the exposure time for sulphuric species will be order of magnitudes longer; for such conditions the sulphation of condensed potassium chloride is no longer negligible [84].

4.3.2 Homogenous alkali sulphation

The alternative route is thus that the sulphation is governed by homogenous gas phase reactions and that K_2SO_4 is condensed soon after its formation. This is a theory which is in agreement with a series of experimental studies [58, 59, 81, 89, 90].

The sulphation of KCl may follow one of the routes shown in Figure 12 including reactions with both SO_2 and SO_3. Regardless of the route, the final step is the condensation of gaseous K_2SO_4, which is formed in reaction of $KHSO_4$ and KCl or KOH,

$$KHSO_4 + KCl \rightleftharpoons K_2SO_4 + HCl \quad \textbf{R 4}$$
$$KHSO_4 + KOH \rightleftharpoons K_2SO_4 + H_2O \quad \textbf{R 5}$$

There are mainly four routes for formation of $KHSO_4$ including either SO_2 or SO_3. SO_3 may react in a direct reaction with KOH,

$$KOH + SO_3(+M) \rightleftharpoons KHSO_4(+M) \quad \textbf{R 6}$$

or through a two-step reaction starting with KCl,

$$KCl + SO_3(+M) \rightleftharpoons KSO_3Cl(+M) \quad \textbf{R 7}$$
$$KSO_3Cl + H_2O \rightleftharpoons KHSO_4 + HCl \quad \textbf{R 8}$$

$KHSO_4$ may then be formed via SO_2 in a three step reaction starting with K,

$$K + SO_2 \rightleftharpoons KSO_2 \quad \textbf{R 9}$$
$$KSO_2 + O_2(+M) \rightleftharpoons KSO_4(+M) \quad \textbf{R 10}$$
$$KSO_4 + H_2O \rightleftharpoons KHSO_4 + OH \quad \textbf{R 11}$$

or starting with KSO_3, which can be formed from either KO (involving SO_2) or K (involving SO_3).

$$KSO_3 + OH \rightleftharpoons KHSO_4 \quad \textbf{R 12}$$
$$KO + SO_2 \rightleftharpoons KSO_3 \quad \textbf{R 13}$$
$$K + SO_3(+M) \rightleftharpoons KSO_3(+M) \quad \textbf{R 14}$$

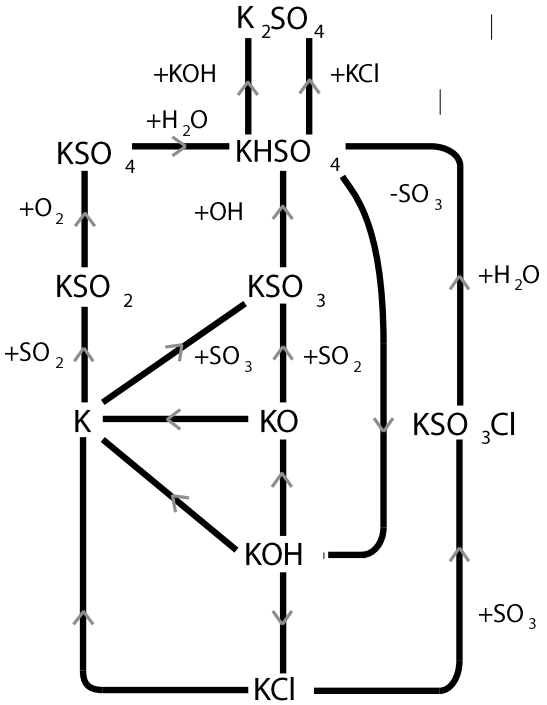

Figure 12. Illustration describing the main reactions during sulphation of KCl.

KCl, KOH, KO and K are the basis for the sulphating process. These compounds are linked together via several reactions of which the most important are given below. KOH may form from KCl via a reaction with water,

$$KCl + H_2O \rightleftharpoons KOH + HCl \quad \textbf{R 15}$$

KOH may react further to KO,

$$KOH + OH \rightleftharpoons KO + H_2 \quad \textbf{R 16}$$

K is formed directly from KCl via one of the following reactions,

$$KCl(+M) \rightleftharpoons K + Cl(+M) \quad \textbf{R 17}$$
$$KCl + H \rightleftharpoons K + HCl \quad \textbf{R 18}$$

or indirect via KOH or KO,

$$KOH + H \rightleftharpoons K + H_2O \quad \textbf{R 19}$$
$$KOH(+M) \rightleftharpoons K + OH(+M) \quad \textbf{R 20}$$
$$KO + O \rightleftharpoons K + O_2 \quad \textbf{R 21}$$
$$KO + CO \rightleftharpoons K + CO_2 \quad \textbf{R 22}$$
$$KO + SO_2 \rightleftharpoons K + SO_3 \quad \textbf{R 23}$$

The present work focuses entirely on this suggested route with homogenous alkali sulphation, as described by the reaction path schematic shown in Figure 12. Thus, this forms the basis for the modelling of the alkali chemistry in both the appended papers as well as for the results presented later on in this thesis introduction.

4.4 CO-interactions

The oxidation of CO (R 24) may be influenced by alkali and chlorine containing species as well by SO_2. The inhibiting effect has been experimentally observed for both hydrogen [91-94] and hydrocarbon–air flames [67, 95-102] (both in laboratory scale), for HCl and SO_2 it has also been reported for PC combustion [103] and finally the phenomenon has also been examined for various conditions in flow reactors[104-107]. The interaction may either be direct or via the O/H radical pool which is important for the chain branching driving the combustion. Below follows a theoretic discussion on how these compounds may affect the oxidation of CO. The reactions discussed form the basis for the kinetic modelling carried out in Paper II.

$$CO + OH \rightleftharpoons CO_2 + H \quad \textbf{R 24}$$

4.4.1 Sulphur-CO interactions

It is well known that SO_2 can influence the combustion chemistry, and, depending on the local air to fuel ratio its presence can either inhibit or pronounce the oxidation of CO [30]. During fuel lean conditions a small fraction of SO_2 can be oxidized to SO_3, the latter which also can be reduced back to SO_2 via a second path,

$$SO_2 + O(+M) \rightleftharpoons SO_3(+M) \quad \textbf{R 1}$$
$$SO_3 + O \rightleftharpoons SO_2 + O_2 \quad \textbf{R 25}$$

SO_2 has the largest effect in a reducing relative to an oxidizing environment [69]. Rasmussen et al. [30] has presented a more complex SOx-cycle which has a better agreement for both rich and lean conditions including HOSO.

$$SO_2 + H(+M) \rightleftharpoons HOSO(+M) \quad \textbf{R 26}$$
$$HOSO + H \rightleftharpoons SO + H_2O \quad \textbf{R 27}$$
$$SO + O_2 \rightleftharpoons SO_2 + O \quad \textbf{R 28}$$

They also introduced a third loop including SO for better accuracy during flame combustion (higher temperatures).

$$SO + H(+M) \rightleftharpoons HSO(+M) \quad \textbf{R 29}$$
$$HSO + H \rightleftharpoons S + H_2O \quad \textbf{R 30}$$
$$S + OH \rightleftharpoons SO + H \quad \textbf{R 31}$$

Despite this more complex SOx-cycle presented by Rasmussen et. al [30] there are still some sulphur-fuel interactions that are not yet captured by the mechanism [69].

4.4.2 Alkali-CO interactions

Alkali species in a combustion facility can be found both as solids and in the gas phase. However, the inhibiting effect on CO oxidation has been shown for both physical states. The influence of alkali species are referred to be due to chemical interactions whereas more chemically inert solids, such as silica powders, rather have a thermal influence [97, 102]. Even though the details of the chemical mechanism behind this phenomenon is still being discussed in the literature it is most often suggested to be based on reactions in the gas phase [69, 99, 101, 104, 108]. Based on gas-phase experiments in previous studies [67, 93, 94, 99, 104, 109] a mechanism including reactions (**Error! Reference ource not found.-Error! Reference source not found.**) has been suggested; interactions via the O/H radical pool connects the CO oxidation (R 24) with the potassium available in the gas phase.

$$K + OH + M \rightleftharpoons KOH + M \quad \textbf{R 20}$$
$$KOH + H \rightleftharpoons K + H_2O \quad \textbf{R 19}$$
$$KCl + H \rightleftharpoons K + HCl \quad \textbf{R 18}$$
$$KCl + H_2O \rightleftharpoons KOH + HCl \quad \textbf{R 15}$$

In order for these reactions to describe the observed inhibiting effect the reaction rate for (**Error! eference source not found.**) has to be higher than what has been confirmed. Hynes et. al [91] proposed an additional reaction involving KO_2 to an additional reaction enabling the reaction rate to be lower but it seems unlikely according to the thermodynamic properties found for alkali dioxides [104]. Potassium containing compounds has been reported to able to both inhibit CO oxidation in an oxygen rich environment and to promote CO oxidation under certain conditions e.g. in the presence of high NOx concentrations[110, 111].

4.4.3 Chlorine-CO interactions

Chlorine containing species is released already during the pyrolysis and is mainly found in the gas phase as chlorinated hydrocarbons, HCl or KCl [68, 69]. In the same way as for the alkali metals chlorine interacts with the CO oxidation via the O/H radical pool in a cycle of reactions as follows [69, 105]

$$HCl + H \rightleftharpoons Cl + H_2 \quad \textbf{R 32}$$
$$HCl + OH \rightleftharpoons Cl + H_2O \quad \textbf{R 33}$$
$$Cl + H + M \rightleftharpoons HCl + M \quad \textbf{R 34}$$
$$Cl + HO_2 \rightleftharpoons HCl + O_2 \quad \textbf{R 35}$$

There is also a second cycle including CO directly [112]

$$Cl + HO_2 \rightleftharpoons ClO + OH \quad \textbf{R 36}$$
$$ClO + CO \rightleftharpoons Cl + CO_2 \quad \textbf{R 37}$$

The relation between these two cycles depend on whether the reaction between $Cl + HO_2$ will follow (R 35) or (R 36). This is especially important, as the first route will inhibit while the second will promote CO oxidation. The inhibiting effect of the first cycle might also be reduced or changed to promoting conditions in areas with higher Cl concentrations (e.g. the post flame zone) forcing (R 32) and (R 33) to reach equilibrium or even change to the reverse reaction [69].

5 Results

As presented in detail in the method section, KCl and SO_2 was injected into the 80 kW propane flame with the aim to isolate the related alkali sulphation chemistry, i.e. without interaction with other inorganic components typically found in ashes from solid fuels. In the present chapter results from combustion experiments and modelling on the alkali sulphation behaviour in air and oxy-fuel atmospheres (related mainly to paper I) and the chemical interaction between K, Cl and S-components with the CO oxidation in flames (Paper II).

5.1 Sulphation of KCl

The experimental results (Air and OF25) presented in Figure 13 are compared with the modelling results (Air_M and $OF25_M$). The degree of sulphation is presented in Figure 13a and b as a function of the S/K-ratio in the flue gas and injected respectively. The sulphation during air combustion is independent of the two ways of presenting the S/K-ratio. The degree of sulphation in the oxy-fuel cases, on the other hand, depends on how the ratio is defined due to the flue gas recirculation. A comparison of Figure 13 a and b shows that the degree of sulphation is enhanced during oxy-fuel combustion compared to air combustion, i.e. independent of how the S/K ratio is defined. However, the difference between air and oxy-fuel combustion is larger with respect to the S/K ratio injected (Figure 13 b). The trend with an enhanced sulphation for increasing S/K-ratio is captured by the model. However, there are some deviations especially for OF25 and $OF25_M$. The measured values with over 100 % sulphation are possibly a result of deposited KCl being sulphated.

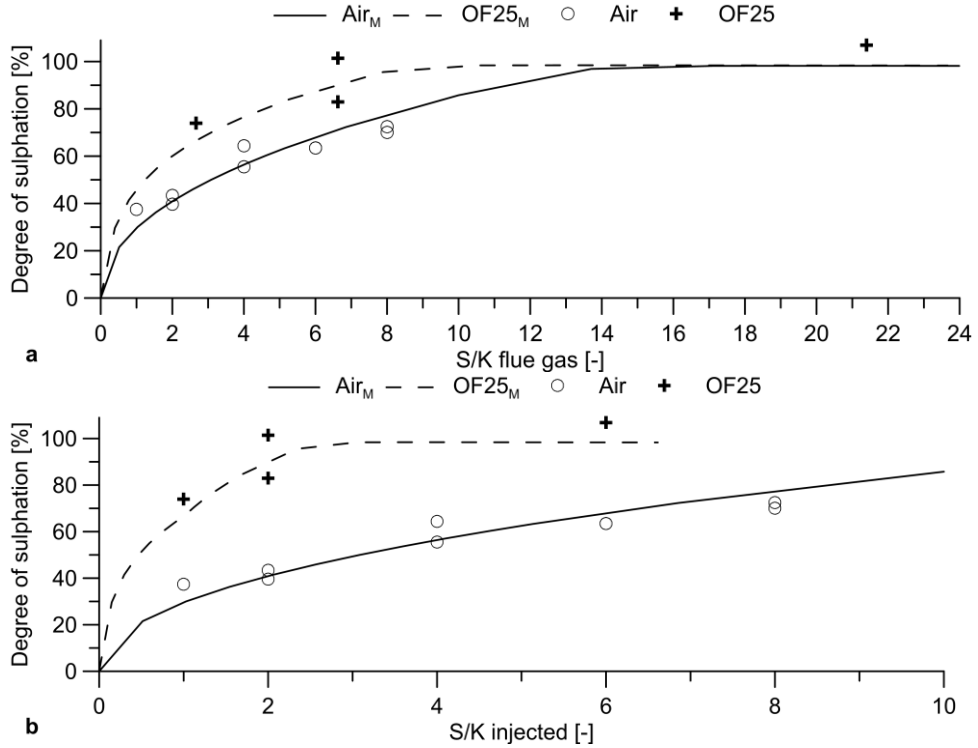

Figure 13. Modelling and experimental results for the degree of sulphation in the Air and OF25 cases at different a) S/K in the flue gas, and b) S/K in the fuel.

The SO_3 concentration was measured at the combustor exit (M8) for air and OF25 conditions with and without KCl injection; the same SO_2 injection was kept for both cases with and without KCl presented in Figure 14. The measured concentration of SO_3 for low S/K ratios does not follow the same trend as for higher S/K ratios. However, it is clear that the injection of KCl lowers the SO_3 concentration, which is seen in all cases regardless of the combustion environment investigated.

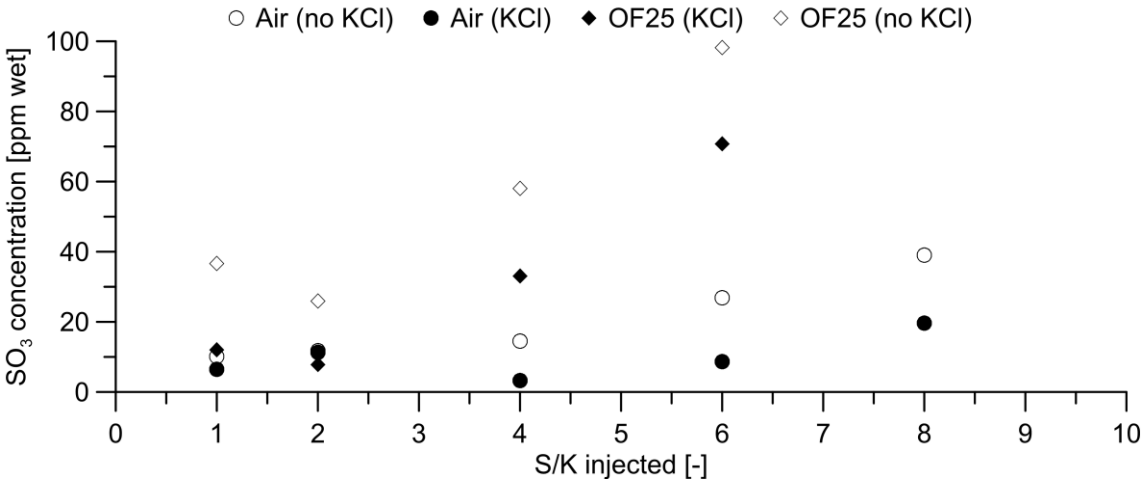

Figure 14. The SO_3 concentration measured in port 8 for Air and OF25. During the "no KCl" cases the SO_2 concentration in the oxidiser is kept the same as in the case with KCl injection.

A reaction path analysis of potassium compounds during sulphation of KCl is presented in Figure 15. The figures demonstrate the difference in reaction activity (see section 3.4, Data evaluation, for definition of the reaction activity) between the three cases: Air_{FG}, $OF25_{FG}$ dry and $OF25_{FG}$ wet. The overall reaction activity is highest in the $OF25_{FG}$ dry case even though the formation of K_2SO_4 is not that much higher than in the $OF25_{FG}$ wet case. The Air_{FG} case has the lowest reaction activity of the three. Note that reaction (R 6) ($KOH + SO_3(+M) \rightleftharpoons KHSO_4(+M)$) acts as a source to SO_3 formation in all cases.

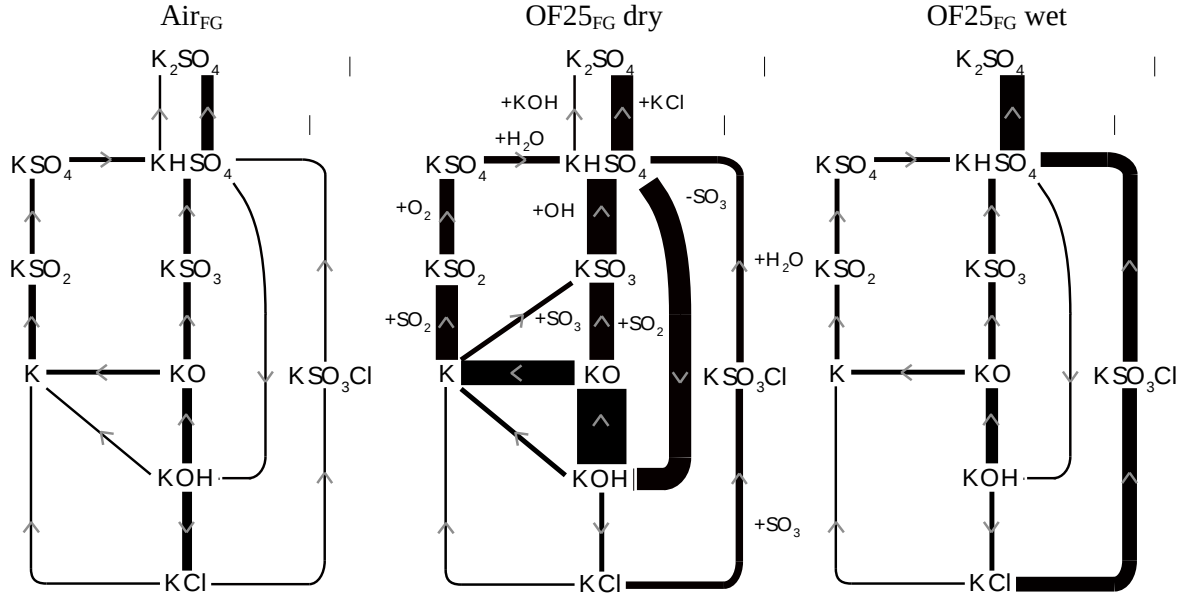

Figure 15. Modelling results of the activity for important reaction paths during sulphation of KCl in flue gases from the Air_{FG}, $OF25_{FG}$ dry and $OF25_{FG}$ wet cases. Only reactions containing potassium are shown. The relative thickness of each line indicates the activity of each individual path normalized with respect to the overall highest activity for all three cases. Source: Paper I.

As indicated in the reaction path analysis (Figure 15) some reactions in the sulphation process involves SO_2 while others are based on SO_3. The relative importance varies depending on the flue gas composition as can be seen in Figure 16. More than 50% of the K_2SO_4 formed in the $OF25_{FG}$ wet case can be attributed to reactions involving SO_3. This is almost three times the amount formed via SO_3 in the Air_{FG} and $OF25_{FG}$ dry cases. However, the fraction of SO_3 is highest throughout the entire reactor in the $OF25_{FG}$ dry case compared to both the Air_{FG} and $OF25_{FG}$ wet cases. The peak fraction for both oxy-fuel cases are higher than the fraction found in the air derived flue gases, almost 10 and 6 times higher respectively. On the other hand, all SO_3 is consumed in both the Air_{FG} and $OF25_{FG}$ wet cases whereas the exit fraction is almost 20 ppm in the $OF25_{FG}$ dry case.

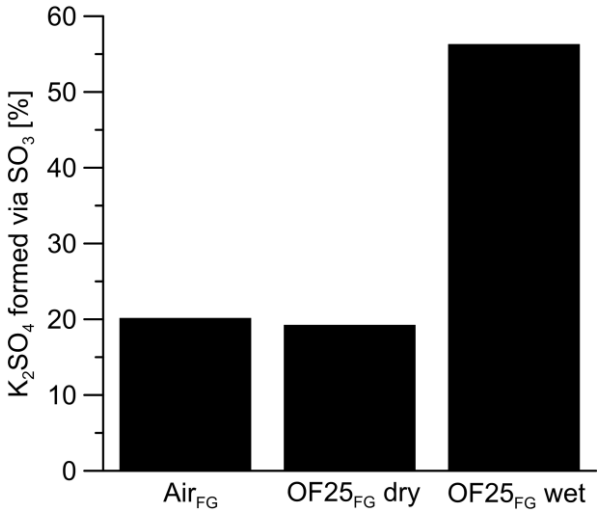

Figure 16. Percentage of the total amount of K_2SO_4 formation via reactions including SO_3 for all cases. Source: Paper I.

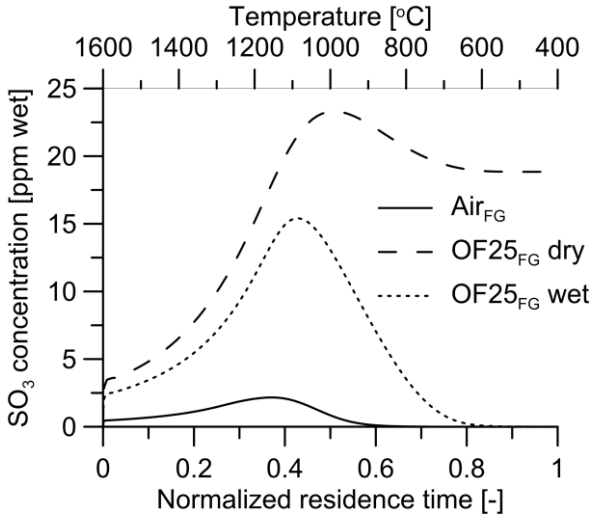

Figure 17. Variations in SO_3 concentration throughout the reactor for all three flue gas cases investigated. Source: Paper I.

Figure 18 shows photos of the flame with and without KCl injection for the Air (Figure 25a and b respectively) and the OF25 case (Figure 25c and d respectively). The photos of the Air flame are taken in port M2 while the OF25 photos are taken further downstream in M3. The change in colour is due to the KCl injection and from a visual observation the KCl seems evenly distributed within the flame already in port M2 (air flame).

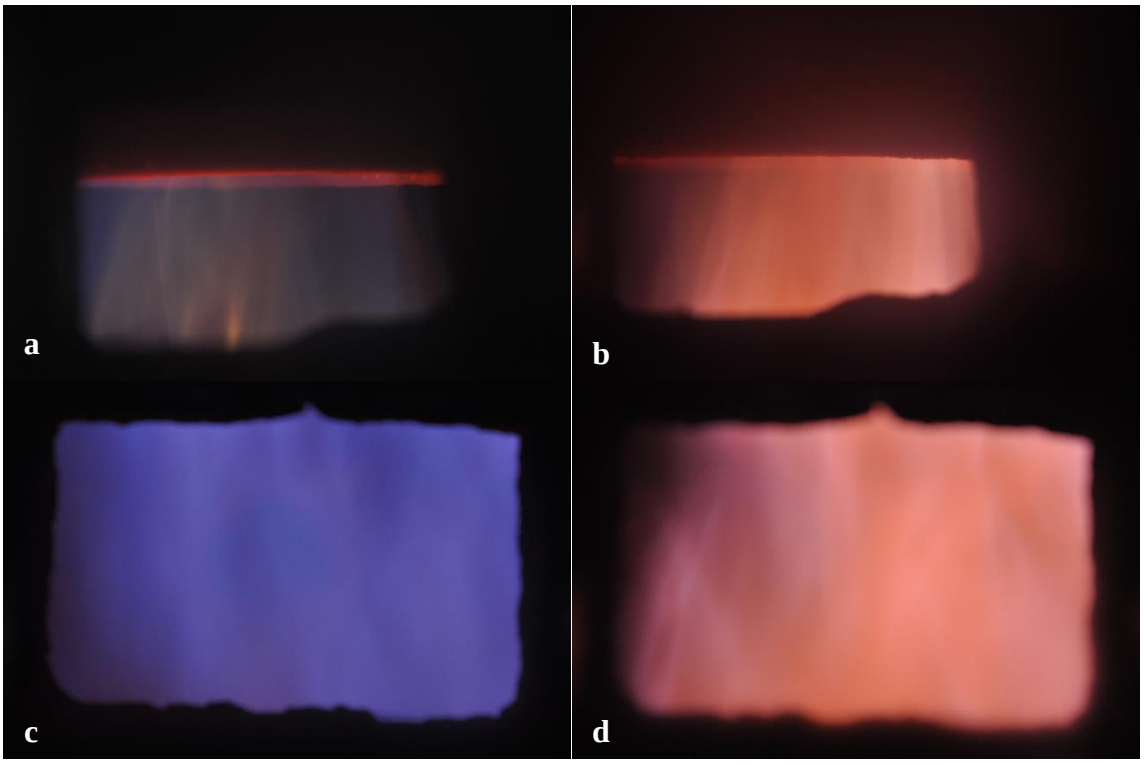

Figure 18. Pictures of the flame taken during operation. The Air case both without and with KCl injection is shown in a) and b) respectively, both pictures taken in measurement M2. The OF25 case is shown in c) and d) with out and with KCl injection. The OF25 pictures are from M3. Source: Paper II.

Figure 19 resents the measured HCl concentration before the KCl injection was started and after injection (the injection starts at t=200s). The concentration profile shows a clear increase in HCl level when the injection is started. It is also shown that the HCl concentration drops as soon as no more KCl is injected to the system (600-700s). The obtained HCl concentration when the KCl injection has stopped is slightly higher than before the injection was started. When HCl is measured in a system completely free from HCl the instrument indicates 0-3 ppm. To reach this level again, after KCl has been injected, required several hours of operation and a slight increase in "background" signal was therefore accepted. However, it should be noted that after a full day of experiments the background level was never above 15 ppm. Worth noting is also that the required time to reach a HCl concentration lower than 3 ppm, was drastically shortened when the SO_2 injection was stopped. When the injection was started again the HCl level increased which suggests that some KCl may have formed deposits which were slowly sulphated resulting in a detectable amount of HCl. In the experimental work, only measurements with a significant increase in HCl concentration, as a result from the KCl injection, has been considered accurate.

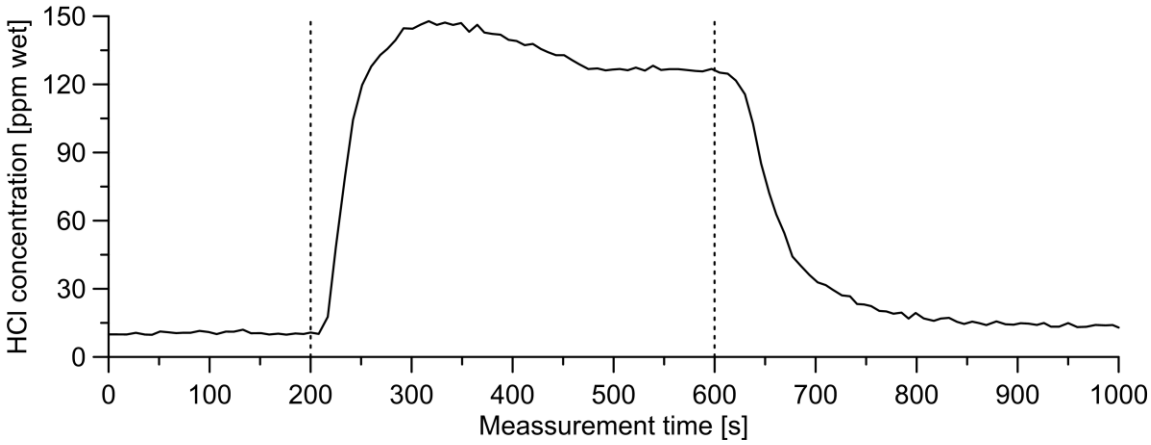

Figure 19. Logged HCl concentration before and after the start of injection of KCl.

As a part of this work, aerosol measurements were conducted using a SMPS, VT-DMA and a DLPI. A result from the VT-DMA measurement is shown in Figure 20. The measurement was performed for the Air case in a centre position of port M3 and compares the relative volume fraction for 80 nm particles during KCl injection together with data for combined injection of KCl and SO_2. The monodisperse particle stream of 80 nm has been heated up before the size distribution is measured again making it possible to see if there is a change caused by the increased temperature. This relative loss in volume is presented for temperatures between 400°C and 800°C in Figure 20. The main volume loss both with and without SO_2 injection occurs between 475°C and 550°C, but in the case of both KCl and SO_2 injection about 6.7 % of the mass is still measured for temperatures above 600°C. The remaining volume found at these temperatures indicates that something else than KCl has been detected – presumably K_2SO_4 – which has a much higher evaporation temperature compared to KCl. If the measurement had included higher temperatures it would have been easier to classify the remaining mass. Measurement port M3 is relatively close to the burner and this should thus be an early stage of the sulphation which is also the case. If the entire volume is assumed to remain as K_2SO_4 at temperatures above 600°C result in a degree of sulphation of 7.6 %.

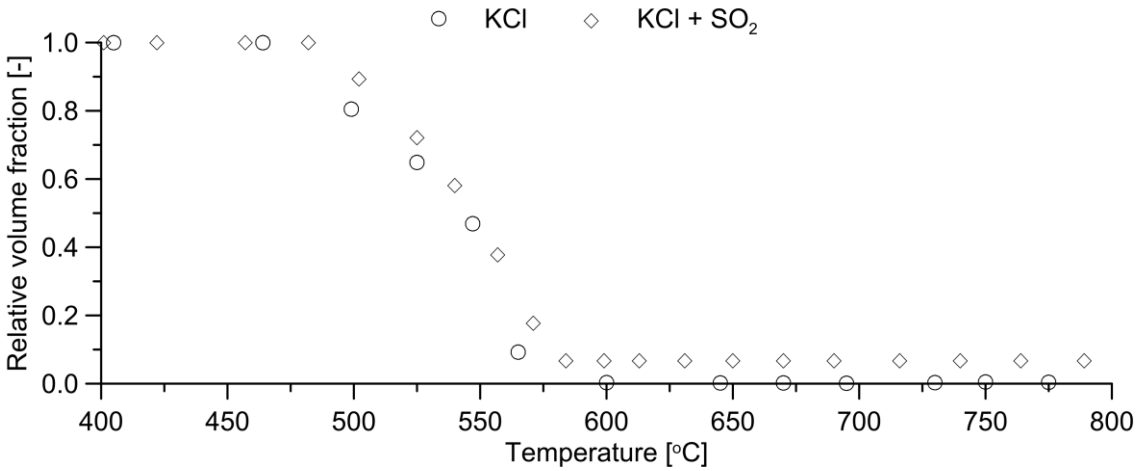

Figure 20. Relative volume fraction measured with a VT-DMA in port 3, centrum position, during air-fuel combustion during KCl injection with and without SO_2 injection. The measurement was performed for particles with a diameter of 80 nm.

By using a DLPI it is possible to collect the sampled particles (in this case soot and potassium containing aerosols) in 13 different size ranges. By weighing the foils before and after the particle sampling particle concentration and size distribution (by mass) can be calculated. Unfortunately an accurate weighing could not be performed due to errors during the reference weighing. However,

photos of the first nine stages (d_{50} 30 nm to 1060 nm) from measurements during injection of KCl can be seen in Figure 21. From these photos a clear visual difference can be observed between the individual stages. There are visible aggregates of particles on stage one to five. The aggregates are not that pronounced on stage six and seven and on stage eight and nine there is only a white thin layer which is difficult to see on the photos. The white layer can be found to varying extent on all the higher stages. The aggregates are darker and larger on the plates used during measurements without KCl injection. In addition, the white thin layer was not found on the foils from the experiments which did not include KCl injection. The layer is therefore believed to be a result of salt condensation or condensation of water when the DLPI is cooled. Judging from the pictures most of the particles seem to be smaller than 400 nm. DLPI measurements give no information of the composition of the particles and additional analysis by for example SEM-EDX would thus be required to determine the composition. In this way soot can be distinguished from the alkali aerosols. The combination of DLPI measurements and SEM EDX analysis will be considered in future experiments.

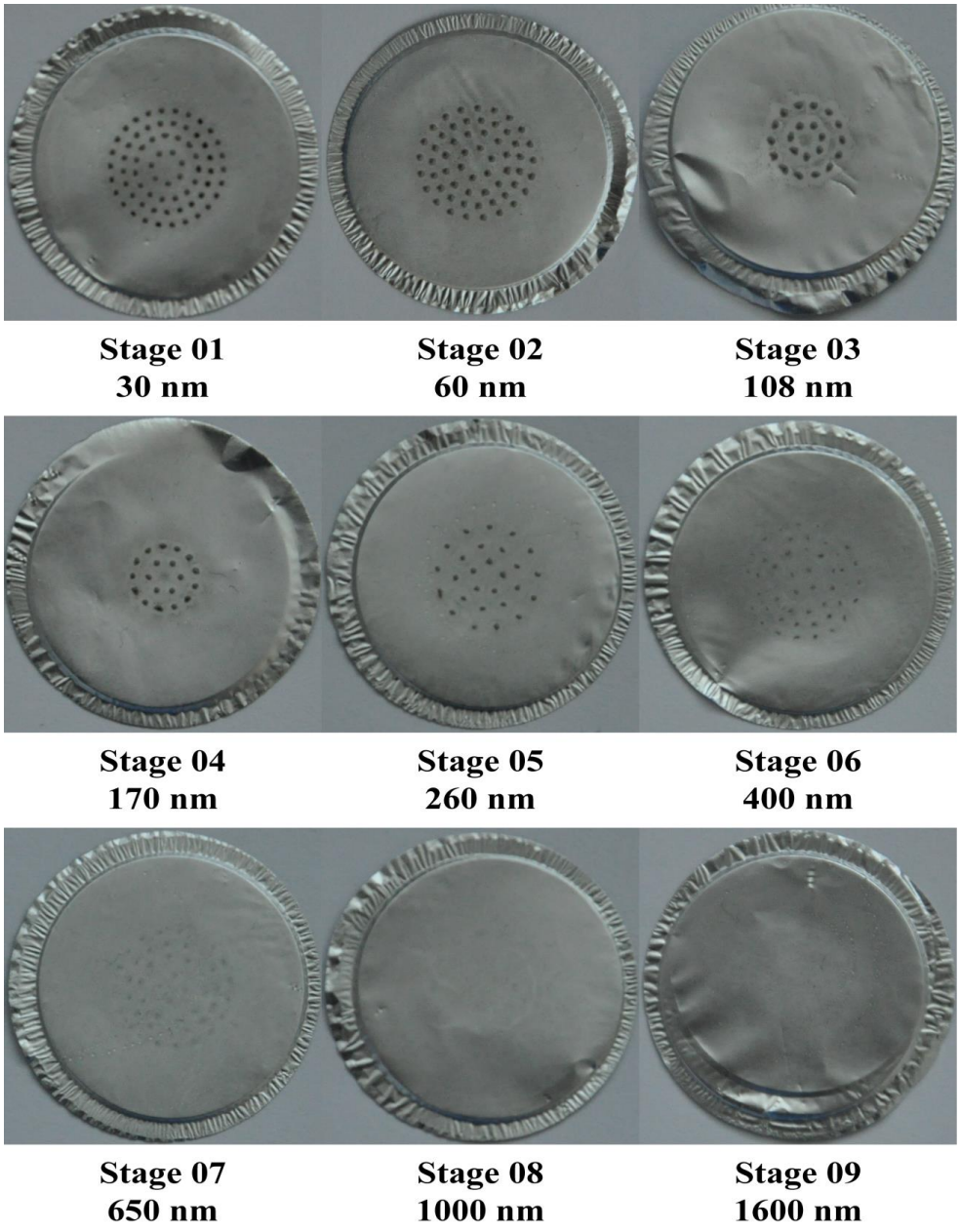

Figure 21. Pictures of the collecting foils used for the nine first stages in the DLPI during injection of KCl in to the flame.

5.1.1 Sensitivity analysis

A modelling based sensitivity analysis was carried out to examine the alkali sulphation behaviour in air and oxy-fuel atmospheres for a wide range of conditions with respect to flue gas composition and temperature (see details in Paper I). In the sensitivity analysis three cases are investigated where the gas atmosphere is altered (N_2-base, CO_2-base, and, CO_2/H_2O-base). The degree of sulphation is favoured by a high inlet SO_2 concentration (high S/K-ratio) as shown in Figure 22a. The CO_2/H_2O case reaches a level close to 100 % at an approximate S/K-ratio of 6 after which it remains stable for higher ratios. In order to achieve complete sulphation the S/K-ratio has to be 10 for the two other test cases. All three cases are also favoured by a higher O_2 fraction although the effect is less prominent compared to the influence of the S/K-ratio. No significant difference is shown between the N_2 and the CO_2 case. The CO_2/H_2O case shows a higher degree of sulphation for all O_2 fractions investigated (Figure 22b). In comparison to the O_2 fraction and the S/K-ratio the HCl/KCl- ratio has an inhibiting effect on the sulphation process already at low fractions (lower than 2), see Figure 22c. The degree of sulphation decreases for higher HCl/KCl ratios but with an asymptotic value of about 5% which is reached already at a ratio of 3; the difference between the three cases is negligible.

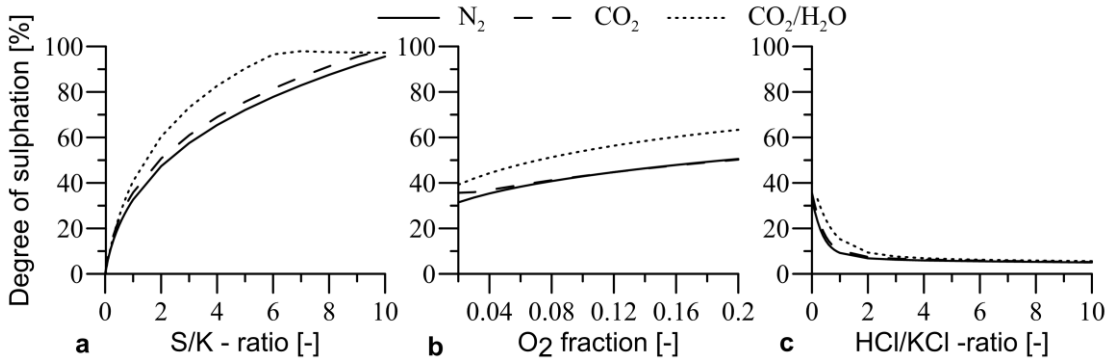

Figure 22. Degree of sulphation of KCl for N_2-, CO_2- and CO_2/H_2O-based atmospheres as a function of a) inlet S/K-ratio, b) inlet O_2 fraction and c) inlet HCl/KCl-ratio. Source: Paper I

The sulphation is active between 700°C and 1300°C with a peak around 1100°C (Figure 23) independent of flue gas atmosphere, although the peak for the CO_2/H_2O atmosphere is higher and also slightly wider, Figure 23a. Also a higher sulphur level causes a wider sulphation peak (Figure 23 b). The presence of HCl, however, lowers the degree of sulphation and shifts the temperature interval of sulphation towards lower temperatures.

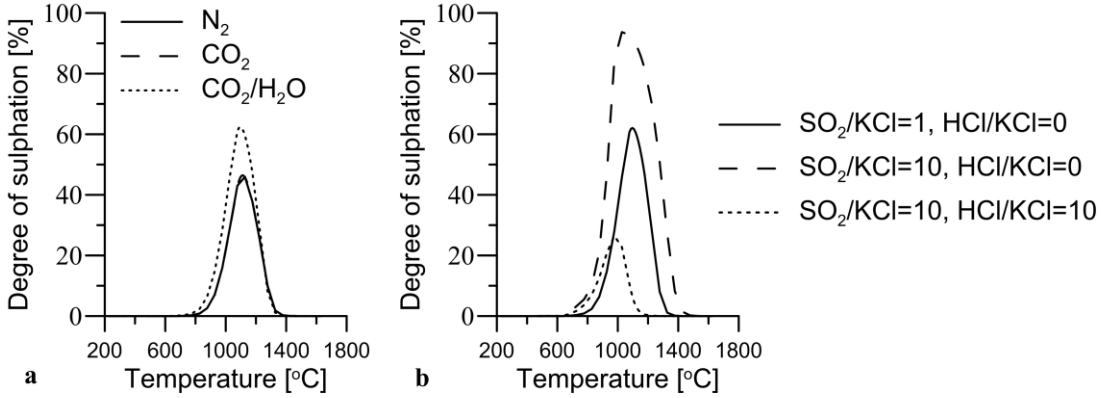

Figure 23. Degree of sulphation for isothermal conditions. a) the solid, dashed and dotted line represent a N_2, CO_2 and CO_2/H_2O-based atmosphere, respectively. b) The solid, dashed and dotted line represent a CO_2 atmosphere with different SO_2/KCl and HCl/KCl ratios. Source: Paper I.

Figure 24 compares the degree of sulphation when equilibrium is reached at various temperatures in the CO_2 rich atmosphere (a) and in a modified CO_2-rich case with higher sulphur and HCl contents (b). The N_2 and CO_2/H_2O case are not shown since the results were similar to the CO_2 rich case. The equilibrium favours complete sulphation at temperatures lower than 900°C where the reaction instead is kinetically limited. The reaction rate is sufficiently high for the sulphation to take place during a residence time of 4 seconds; the sulphation activity is on-set in a temperature window between 800°C and 1300 °C (the case in Figure 24a). When the sulphur and chlorine contents increase, the sulphation reaction rate decreases and the maximum reaction rate is shifted towards lower temperatures, with a temperature reduction of about 200°C. The equilibrium driven sulphation is also shifted towards lower temperatures as can be seen by comparing Figure 24a and b.

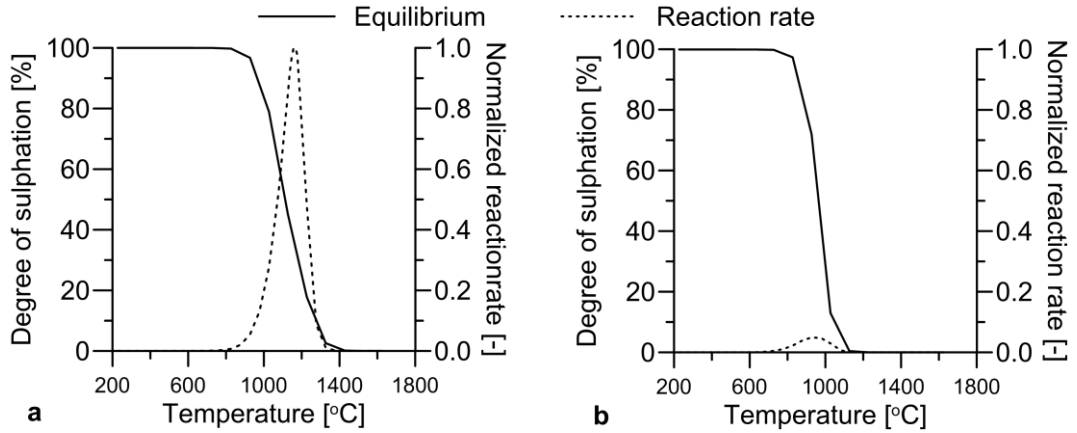

Figure 24. a) Degree of sulphation when equilibrium is reached for temperatures between 500 K and 1900 K for a CO_2 atmosphere. Also the reaction rate in reaction (R 4) and (R 5) is shown for the same temperature interval. b) The same as in a) but for a CO_2 case with S/K ratio and Cl/K ratio of 10. The reaction rates shown are normalized with respect to the maximum reaction rate in the case without HCl (figure a).

5.2 K, Cl and S interactions with CO-oxidation

Figure 25 gives the measured CO concentration along the furnace centre-line at different levels in the furnace. Figure 25a shows the results from air-fuel combustion with different additives injected via the burner or via the oxidant as described previously. As shown, no significant change in CO concentration can be observed for any of the injected additives. The CO concentration declines with an increasing distance from the burner until the oxidation is almost complete at a burner distance of 800 mm. The concentrations measured close to the burner (215 mm) suggest a slightly lower concentration of CO when KCl is injected.

Figure 25b shows that the measured CO concentration in general is higher in oxy-fuel compared to air-fuel combustion. The figure also indicates that the CO oxidation is completed faster. Also, during oxy-fuel operation the effect on CO-oxidation when KCl is injected is more significant. As seen, all cases without KCl injection exhibit a higher concentration in relation to those including KCl in every position from the burner inlet up to a distance of 800 mm when the oxidation is complete. The effect on the measured CO concentration is substantial in the case when the amount of injected KCl is doubled. However, despite this demonstrated effect by the KCl injection on the in-flame CO concentration, the total time for CO oxidation remains in principle the same with and without KCl injection.

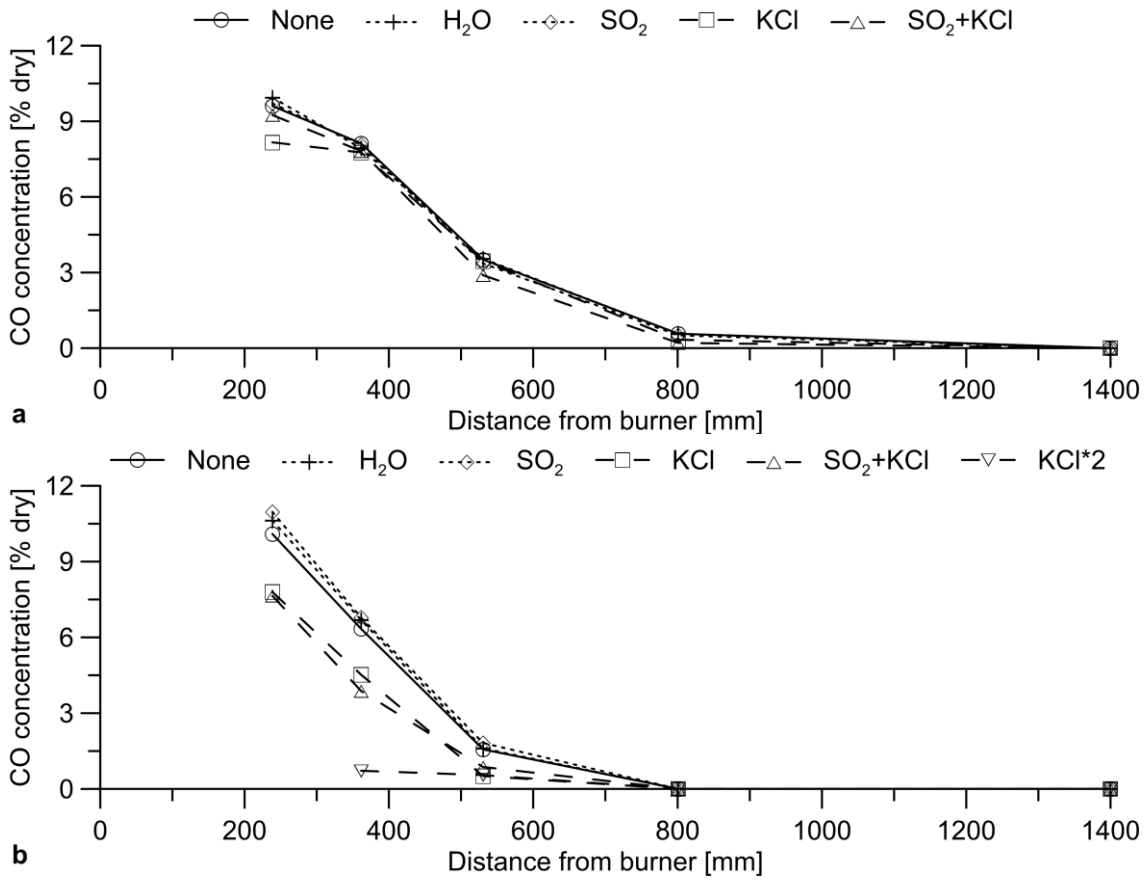

Figure 25. CO concentrations for Air (a) and OF25 (b) with and without injection of KCl SO_2 and water. An additional case is added (KCl*2) for the OF25 case in which the amount of KCl injected is doubled (1.8 l/h). Source: Paper II.

During oxy-fuel combustion, the injection of KCl also influences the SO_2 concentration, as shown in Figure 26. In Figure 26a, the concentration of SO_2 increases soon after the KCl injection is started while at the same time the CO concentration is reduced. According to the results presented in Figure 26b the SO_2 concentration is lower during KCl injection close to the burner and approaches the same value further downstream when the fuel oxidation process is completed.

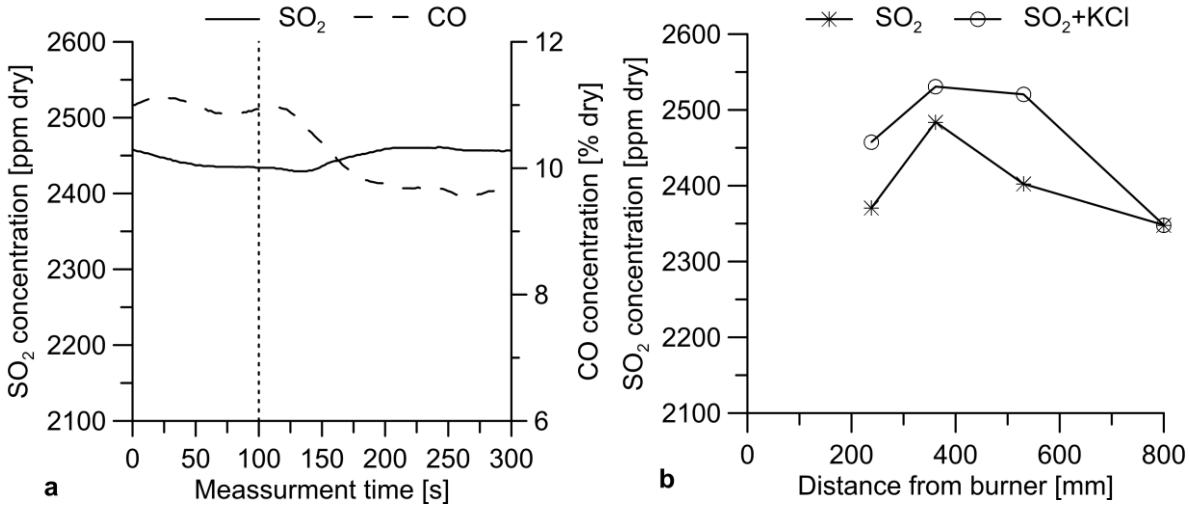

Figure 26. a) SO_2 and CO concentration prior to and after the start of KCl injection (time 0 s). b) SO_2 concentration profiles along the centreline both with and without KCl injection. Source: Paper II

5.2.1 Sensitivity analysis

In Figure 27, the effect of KCl on the CO oxidation for different temperature conditions and CO_2 concentrations is shown. This figure compares the outlet concentration of CO in a system free from KCl with the same where KCl is present (see Table 4 for details). In the case when $CO_{outet}^{KCl}/CO_{outlet} > 1$, KCl has an inhibiting effect on the oxidation (no colour in the figure) If the ratio is less than one, KCl has an oxidizing effect (dark grey in the figure), and, if the ratio is equal to one KCl has no effect on the CO oxidation (light grey in the figure). A CO_2 concentration above 10% will cause a temperature interval where KCl promotes CO oxidation. It also shows that this temperature interval changes towards lower temperatures for higher CO_2 concentrations.

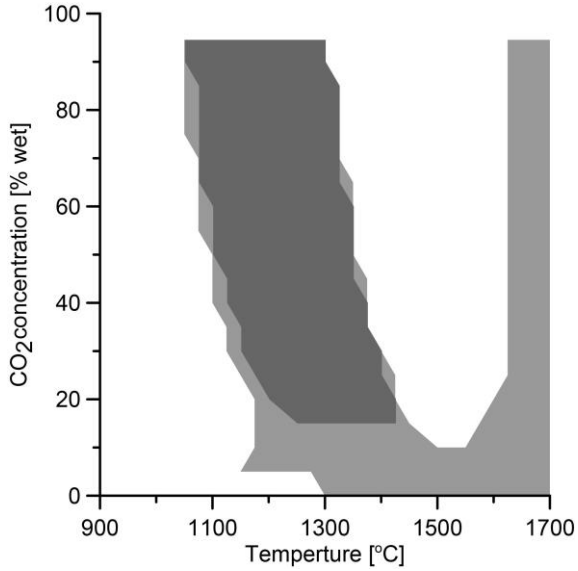

Figure 27. A CO_2-temperature map describing the relative effect of KCl on the CO concentration. Source: Paper II.

6 Discussion

6.1 K-Cl-S Chemistry

According to the results presented in this thesis (cf. Figure 13), the degree of sulphation is higher for oxy-fuel combustion compared to air-fuel combustion for the same S/K-ratio. As a result of the flue gas recirculation, the SO_X concentrations found in oxy-fuel derived flue gases are high compared to flue gases from air combustion (Figure 14 and Figure 17). This leads to enhanced sulphation in oxy-combustion (Figure 22a). The higher sulphur content is, however, not the only explanation as can be seen in Figure 13 where the degree of sulphation is higher in oxy-fuel compared to air-fuel conditions also for similar S/K-ratios in the flue gas. The possible sulphation enhancement due to a shift from N_2 to CO_2 base atmosphere, or the increased O_2 concentration in the OF25 case compared to air, is according to the sensitivity analysis (Figure 22 b and c) too small to be responsible for the difference found between oxy-fuel and air combustion. Temperature has also been shown to be of importance and during the combustion simulations the exact same temperature profiles were used for air and oxy-combustion. Due to the reduced volumetric flow in OF25 compared to Air, this pre-set temperature profile caused a difference in the relation between residence time and temperature. Figure 24 indicates that the sulphation might be limited by kinetics and equilibrium at different temperatures and the residence time-temperature relation may thus be of importance where the process is kinetically controlled. Additional experimental data is required in order to further examine these effects, both for air and oxy-fuel combustion atmospheres.

The ratio between SO_2 and SO_3 is suggested to be important for the homogenous sulphation of alkali metals [62, 113]. In this work an increased SO_3 concentration (Figure 14) was measured when more SO_2 was introduced to the flame while lower concentrations of SO_3 were measured in the presence of KCl, as expected. In the flue gas simulations the estimated SO_3 concentration was lower compared to the measured concentrations; for the Air_{FG} and $OF25_{FG}$ wet case calculations, no SO_3 was detected at the outlet (Figure 17). Those simulations also show a higher relative formation of K_2SO_4 via SO_3 during wet flue gas recirculation in relation to the other two cases (Figure 16 and Figure 17) where the relative formation of potassium sulphate via SO_3 is almost one third of what is found for $OF25_{FG}$ wet. A possible reason is the reaction path via KSO_3Cl, in which water is consumed (R 8), and which is therefore likely to be favoured by higher water concentrations. In a system with relative high water levels in the flue gases, e.g. oxy-fuel applying wet flue gas recirculation or combustion of a fuel with high moisture content (such as pure biomass), the relation between SO_2 and SO_3 might be of greater importance compared to a system with lower water content. SO_3 has been reported by Kassman et al. [54] to increase the degree of sulphation in relation to SO_2 during biomass combustion. Even though the $OF25_{FG}$ dry case exhibits a higher SO_3 concentration compared to the Air_{FG} case the relative sulphation via SO_3 is similar in both environments. The reason may be the water concentration which is similar in both cases.

According to Figure 15, more $KHSO_4$ is formed in oxy-combustion with dry than with wet flue gas recycling. However, overall the difference in degree of sulphation is modest. The reason is the much more active reaction (R 6) which forms significantly more SO_3 in the $OF25_{FG}$ dry case compared to the Air_{FG} and $OF25_{FG}$ wet cases. The increased reaction activity, without further sulphation, suggests

that the system is “saturated” with sulphur. The same result is indicated both in the sensitivity analysis (Figure 22 a) and by the results from the simulations and experiments in Figure 13 where the maximum degree of sulphation is reached at lower S/K-ratios than what is found in the $OF25_{FG}$ dry case.

6.2 CO-oxidation

Changing from N_2 to a CO_2 rich environment seems to increase the sensitivity of CO-oxidation to KCl injection. The results (Figure 25 b) show a clear reduction in CO concentration during injection of KCl during oxy-fuel combustion independent of the presence of SO_2. However, most important is that the effect on CO oxidation is increased when the amount of KCl is doubled. Also the sensitivity analysis suggests a possible difference between air and oxy-fuel combustion conditions. The data presented in Figure 27 does obviously not represent the exact same conditions as those examined experimentally but still indicates that the influence of KCl can change from inhibiting to promoting conditions depending on the chemical composition and temperature of the flue gas.

The potassium in KCl tend to form sulphates in the presence of SO_2 which, in contrast to the results, suggests that the concentration of SO_2 should be lower during injection of KCl. However, in this initial phase of the combustion process, there is no significant effect by the sulphation on the overall combustion chemistry. Instead, the less reducing environment, caused by the KCl injection, promotes the sulphur oxidation and the SO_2 formation to some extent.

Figure 25 indicates only a slight increase in the CO concentration in the OF25 case during injection of SO_2. The effect is considered too small to confirm any chemical interaction but it should be noted tha a similar result has been presented by Giménez-López et. al [29]. In their work SO_2 was shown to inhibit CO-oxidation for both N_2 and CO_2 based atmospheres and that the inhibiting effect increases with SO_2 concentration. This may explain why the inhibiting effect was not observed in the Air case or for oxy-fuel cases with a lower SO_2 concentration than what is shown in Figure 25.

A possible influence by the KCl(aq) spray injection on the mixing conditions in the flame is also worth mentioning. The mixing is a limiting step in the oxidation of a fuel during flame combustion. Increasing the mixing would increase the probability for oxygen and fuel/CO to react and hence lowering the CO concentration. The observed effect of KCl on the CO-oxidation could thus be suggested to be due to secondary effect by the KCl(aq) spray on the mixing conditions rather than a chemical effect. If that would have been the case a similar reduction in CO concentration should have been observed also for injection of pure water. During injection of pure water no change or even a slightincrease of the CO concentration was observed.

7 Conclusions

Combustion of biomass and waste for power generation purposes is expected to increase during the coming years since this represents a cost-efficient method to reduce anthropogenic CO_2 emissions. The relatively high content of alkali metals and chlorine found in biomass compared to coal increases the risk for problems related to deposition and high-temperature corrosion (HTC). The related chemistry is therefore important in order to utilize the biomass in the best way possible, i.e. in order to maximize the thermal efficiency in power plants. This work focuses on the K-Cl-S chemistry relevant for combustion in flames, sulphation of KCl and the influence of these species on the CO oxidation. The work includes experiments performed in a 100 kW combustion test unit together with kinetic modelling performed using CHEMKIN PRO.

Sulphur is mainly found as SO_2 in the flue gas and SO_2 promotes alkali sulphation. Coal has, in general, a higher sulphur content compared to biomass and therefore more alkali sulphates will form when biomass is co-combusted with coal. Alkali sulphates are less problematic with respect to HTC compared to alkali chlorides and it is therefore beneficial to co-combust coal and biomass from an HTC perspective. The concentration of SO_2 will be even higher during oxy-fuel combustion compared to air combustion, and, as a result, the degree of sulphation will typically be higher for oxy-fuel compared to air-combustion, as also observed in our experiments. Thus, the main reason for enhanced sulphation is the higher concentration of SO_2 in oxy-combustion but the relation between temperature and residence time may also contribute to favourable sulphation conditions in oxy-combustion, the latter which requires further analysis in future work.

The relation between SO_2 and SO_3 influences the formation of alkali sulphates. SO_3 may enhance the sulphation but the SO_3 concentration is less important when the overall SO_X concentration is high. A high water concentration has also been shown to favour sulphation via SO_3 which increases the importance of SO_2 oxidation also for high S/K ratios.

Most chlorine is released as KCl in the presence of potassium and otherwise as HCl. HCl has an inhibiting effect on the sulphation already at relatively low concentrations. Wet flue gas recirculation will increase the HCl concentration which thus will reduce the degree of sulphation. Oxy-fuel with wet flue gas recirculation is therefore more sensitive towards the chlorine content in the fuel compared to a system applying dry flue gas recirculation.

When KCl is released during combusting this will not only increase the risk for HTC, it will also influence the oxidation of CO. No significant effect on CO oxidation was detected during the air fired experiments during injection of KCl. However, for oxy-fuel combustiona clear reduction in CO concentration was observed during KCl injection. The observed effect by KCl on the oxidation of CO is, based on our experiments, determined to be a chemical effect rather than a thermal or a mixing effect.

8 Future work

The present work has shown on the potential for an improved control of KCl-induced high-temperature corrosion in oxy-fuel combustion. However, the K-Cl-S chemistry related to sulphation in flue gases has to be further investigated for both air and oxy-fuel combustion. Future experimental work should for example also consider the differences in the temperature-residence time relation between air-fuel and oxy-fuel combustion atmospheres.

The present focuses on the sulphation of pure potassium chloride with experiments conducted in a propane-fired flame. In order to include the full complexity of the real process, combustion of solid fuels containing alkali and sulphur need to be performed. Such an investigation would create a more realistic environment which would include also the effects of e.g. ash retention. In this work, the measurement and modelling results have focused on the gas-phase chemistry. In future experiments, involving solid fuels, other experimental methods will be required to study the sulphation of alkali metals. The aerosol extraction methods, which have been briefly presented in this thesis, show promising results. Also, optical systems, such as IACM (developed for alkali measurements in flue gases) may offer possibilities to measure the sulphation in more complex systems and may also be considered in future work.

9 Bibliography

1. IPCC, *2013: Climate Change 2013: The Physical Science Basis.*, in *Contribution of Working Group I to the Fifth Assessment Report of the Intergovernmental Panel on Climate Change*, T.F. Stocker, D. Qin, G.-K. Plattner, M. Tignor, S.K. Allen, J. Boschung, A. Nauels, Y. Xia, V. Bex and P.M. Midgley, Editor 2013: Cambridge University Press, Cambridge, United Kingdom and New York, NY, USA, 2013. p. 1535.
2. EIA, *U.S. Energy Information Administration: International Energy Outlook 2013*, 2013. p. 312.
3. Wang, M., et al., *Post-combustion CO2 capture with chemical absorption: A state-of-the-art review.* Chemical Engineering Research and Design, 2011. **89**(9): p. 1609-1624.
4. Toftegaard, M.B., et al., *Oxy-fuel combustion of solid fuels.* Progress in Energy and Combustion Science, 2010. **36**(5): p. 581-625.
5. Markström, P., C. Linderholm, and A. Lyngfelt, *Chemical-looping combustion of solid fuels - Design and operation of a 100kW unit with bituminous coal.* International Journal of Greenhouse Gas Control, 2013. **15**: p. 150-162.
6. Bachu, S., *CO 2 storage in geological media: Role, means, status and barriers to deployment.* Progress in Energy and Combustion Science, 2008. **34**(2): p. 254-273.
7. Azar, C., D.J.A. Johansson, and N. Mattsson, *Meeting global temperature targets - The role of bioenergy with carbon capture and storage.* Environmental Research Letters, 2013. **8**(3).
8. Aho, M., T. Envall, and J. Kauppinen, *Corrosivity of flue gases during co-firing Chinese biomass with coal at fluidised bed conditions.* Fuel Processing Technology, 2013. **105**: p. 82-88.
9. Kassman, H., et al., *Two strategies to reduce gaseous KCl and chlorine in deposits during biomass combustion - Injection of ammonium sulphate and co-combustion with peat.* Fuel Processing Technology, 2013. **105**: p. 170-180.
10. Khan, A.A., et al., *Biomass combustion in fluidized bed boilers: Potential problems and remedies.* Fuel Processing Technology, 2009. **90**(1): p. 21-50.
11. Olanders, B. and B.M. Steenari, *Characterization of ashes from wood and straw.* Biomass and Bioenergy, 1995. **8**(2): p. 105-115.
12. Saleh, S.B., et al., *Release of chlorine and sulfur during biomass torrefaction and pyrolysis.* Energy and Fuels, 2014. **28**(6): p. 3738-3746.
13. Andersson, K., et al., *Radiation intensity of lignite-fired oxy-fuel flames.* Experimental Thermal and Fluid Science, 2008. **33**(1): p. 67-76.
14. Andersson, K., et al., *Radiation intensity of propane-fired oxy-fuel flames: Implications for soot formation.* Energy and Fuels, 2008. **22**(3): p. 1535-1541.
15. Andersson, K. and F. Johnsson, *Flame and radiation characteristics of gas-fired O 2/CO 2 combustion.* Fuel, 2007. **86**(5-6): p. 656-668.
16. Fleig, D., et al., *SO 3 Formation under oxyfuel combustion conditions.* Industrial and Engineering Chemistry Research, 2011. **50**(14): p. 8505-8514.
17. Fleig, D., et al. *The fate of sulphur during oxy-fuel combustion of lignite*. 2009.
18. Leckner, B., *Co-combustion - A summary of technology.* Thermal Science, 2007. **11**(4): p. 5-40.
19. Savolainen, K., *Co-firing of biomass in coal-fired utility boilers.* Applied Energy, 2003. **74**(3-4): p. 369-381.
20. Spliethoff, H. and K.R.G. Hein, *Effect of co-combustion of biomass on emissions in pulverized fuel furnaces.* Fuel Processing Technology, 1998. **54**(1-3): p. 189-205.

21. Harb, J.N. and E.E. Smith, *Fireside corrosion in pc-fired boilers.* Progress in Energy and Combustion Science, 1990. **16**(3): p. 169-190.
22. Åmand, L.E., et al., *Ash deposition on heat transfer tubes during combustion of demolition wood.* Energy and Fuels, 2006. **20**(3): p. 1001-1007.
23. Pisa, I. and G. Lazaroiu, *Influence of co-combustion of coal/biomass on the corrosion.* Fuel Processing Technology, 2012.
24. Pettersson, J., J.E. Svensson, and L.G. Johansson, *Alkali induced corrosion of 304-type austenitic stainless steel at 600°C; comparison between KCl, K2CO3 and K 2so4*, 2008. p. 367-375.
25. Pettersson, A., et al. *The impact of zeolites during co-combustion of municipal sewage sludge with alkali and chlorine rich fuels*. 2009.
26. Syed, A.U., N.J. Simms, and J.E. Oakey, *Fireside corrosion of superheaters: Effects of air and oxy-firing of coal and biomass.* Fuel, 2012. **101**: p. 62-73.
27. Fleig, D., K. Andersson, and F. Johnsson, *Influence of operating conditions on SO3 formation during air and oxy-fuel combustion.* Industrial and Engineering Chemistry Research, 2012. **51**(28): p. 9483-9491.
28. Normann, F., et al., *Emission control of nitrogen oxides in the oxy-fuel process.* Progress in Energy and Combustion Science, 2009. **35**(5): p. 385-397.
29. Giménez-López, J., et al., *SO2 effects on CO oxidation in a CO2 atmosphere, characteristic of oxy-fuel conditions.* Combustion and Flame, 2011. **158**(1): p. 48-56.
30. Rasmussen, C.L., P. Glarborg, and P. Marshall, *Mechanisms of radical removal by SO2.* Proceedings of the Combustion Institute, 2007. **31 I**: p. 339-347.
31. Kassman, H., et al., *Measures to reduce chlorine in deposits: Application in a large-scale circulating fluidised bed boiler firing biomass.* Fuel, 2011. **90**(4): p. 1325-1334.
32. Kassman, H., F. Normann, and L.E. Åmand, *The effect of oxygen and volatile combustibles on the sulphation of gaseous KCl.* Combustion and Flame, 2013. **160**(10): p. 2231-2241.
33. Fleig, D., et al., *Evaluation of SO 3 measurement techniques in air and oxy-fuel combustion.* Energy and Fuels, 2012. **26**(9): p. 5537-5549.
34. Maddalone, R.F., et al., *Laboratory and field evaluation of the Controlled Condensation System for SO3 measurements in flue gas streams.* Journal of the Air Pollution Control Association, 1979. **29**(6): p. 626-631.
35. Boman, C., et al., *Characterization of inorganic particulate matter from residential combustion of pelletized biomass fuels.* Energy and Fuels, 2004. **18**(2): p. 338-348.
36. Johansson, L.S., et al., *Particle emissions from biomass combustion in small combustors.* Biomass and Bioenergy, 2003. **25**(4): p. 435-446.
37. Pagels, J., et al., *Characteristics of aerosol particles formed during grate combustion of moist forest residue.* Journal of Aerosol Science, 2003. **34**(8): p. 1043-1059.
38. Valmari, T., et al., *Field study on ash behavior during circulating fluidized-bed combustion of biomass. 1. Ash formation.* Energy and Fuels, 1999. **13**(2): p. 379-389.
39. Wierzbicka, A., et al., *Particle emissions from district heating units operating on three commonly used biofuels.* Atmospheric Environment, 2005. **39**(1): p. 139-150.
40. Strand, M., et al., *Fly ash penetration through electrostatic precipitator and flue gas condenser in a 6 MW biomass fired boiler.* Energy and Fuels, 2002. **16**(6): p. 1499-1506.
41. Wiinikka, H. and R. Gebart, *Critical parameters for particle emissions in small-scale fixed-bed combustion of wood pellets.* Energy and Fuels, 2004. **18**(4): p. 897-907.
42. Valmari, T., et al., *Fly ash formation and deposition during fluidized bed combustion of willow.* Journal of Aerosol Science, 1998. **29**(4): p. 445-459.
43. Strand, M., et al., *Laboratory and field test of a sampling method for characterization of combustion aerosols at high temperatures.* Aerosol Science and Technology, 2004. **38**(8): p. 757-765.
44. Lind, T., et al., *Ash formation mechanisms during combustion of wood in circulating fluidized beds.* Symposium (International) on Combustion, 2000. **28**(2): p. 2287-2294.
45. Wiinikka, H., et al., *High-temperature aerosol formation in wood pellets flames: Spatially resolved measurements.* Combustion and Flame, 2006. **147**(4): p. 278-293.

46. Fernandes, U., et al., *Oxidation behavior of particulate matter sampled from the combustion zone of a domestic pellet-fired boiler.* Fuel Processing Technology, 2013. **116**: p. 201-208.
47. Davis, S.B., et al., *Multicomponent coagulation and condensation of toxic metals in combustors.* Symposium (International) on Combustion, 1998. **2**: p. 1785-1791.
48. McNallan, M.J., G.J. Yurek, and J.F. Elliott, *The formation of inorganic particulates by homogeneous nucleation in gases produced by the combustion of coal.* Combustion and Flame, 1981. **42**(C): p. 45-60.
49. Wiinikka, H., *High Temperature Aerosol Formation and Emission Minimisation during Combustion of Wood Pellets*, in *Applied Physics and Mechanical Engineering*2005, Luleå University of Technology: Applied Physics and Mechanical Engineering. p. 57.
50. Wang, C., et al., *Comparison of coal ash particle size distributions from Berner and Dekati low pressure impactors.* Aerosol Science and Technology, 2007. **41**(12): p. 1062-1075.
51. Biswas, P. and R.C. Flagan, *High-velocity inertial impactors.* Environmental Science and Technology, 1984. **18**(8): p. 611-616.
52. Jiménez, S. and J. Ballester, *Formation and emission of submicron particles in pulverized olive residue (orujillo) combustion.* Aerosol Science and Technology, 2004. **38**(7): p. 707-723.
53. Zeleny, J., *The distribution of mobilities of ions in moist air.* Physical Review, 1929. **34**(2): p. 310-334.
54. De La Mora, J.F., et al., *Differential mobility analysis of molecular ions and nanometer particles.* TrAC - Trends in Analytical Chemistry, 1998. **17**(6): p. 328-339.
55. Park, K., et al., *Tandem measurements of aerosol properties - A review of mobility techniques with extensions.* Aerosol Science and Technology, 2008. **42**(10): p. 801-816.
56. Knutson, E.O. and K.T. Whitby, *Aerosol classification by electric mobility: apparatus, theory, and applications.* Journal of Aerosol Science, 1975. **6**(6): p. 443-451.
57. Hindiyarti, L., et al., *An exploratory study of alkali sulfate aerosol formation during biomass combustion.* Fuel, 2008. **87**(8-9): p. 1591-1600.
58. Iisa, K., Y. Lu, and K. Salmenoja, *Sulfation of potassium chloride at combustion conditions.* Energy and Fuels, 1999. **13**(6): p. 1184-1190.
59. Jensen, J.R., et al., *The Nucleation of Aerosols in Flue Gases with a High Content of Alkali - A Laboratory Study.* Aerosol Science and Technology, 2000. **33**(6): p. 490-509.
60. Jiménez, S. and J. Ballester, *Influence of operating conditions and the role of sulfur in the formation of aerosols from biomass combustion.* Combustion and Flame, 2005. **140**(4): p. 346-358.
61. Jiménez, S. and J. Ballester, *Formation of alkali sulphate aerosols in biomass combustion.* Fuel, 2007. **86**(4): p. 486-493.
62. Li, B., et al., *Post-flame gas-phase sulfation of potassium chloride.* Combustion and Flame, 2013. **160**(5): p. 959-969.
63. Glarborg, P., et al., *Oxidation of formaldehyde and its interaction with nitric oxide in a flow reactor.* Combustion and Flame, 2003. **132**(4): p. 629-638.
64. Glarborg, P., et al., *Kinetic modeling of hydrocarbon/nitric oxide interactions in a flow reactor.* Combustion and Flame, 1998. **115**(1-2): p. 1-27.
65. Alzueta, M.U., et al., *An experimental and modeling study of the oxidation of acetylene in a flow reactor.* Combustion and Flame, 2008. **152**(3): p. 377-386.
66. Abián, M., et al., *Effect of different concentration levels of CO2 and H 2O on the oxidation of CO: Experiments and modeling.* Proceedings of the Combustion Institute, 2011. **33**(1): p. 317-323.
67. Slack, M., et al., *Potassium kinetics in heavily seeded atmospheric pressure laminar methane flames.* Combustion and Flame, 1989. **77**(3-4): p. 311-320.
68. Johansen, J.M., et al., *Release of K, Cl, and S during pyrolysis and combustion of high-chlorine biomass.* Energy and Fuels, 2011. **25**(11): p. 4961-4971.
69. Glarborg, P., *Hidden interactions-Trace species governing combustion and emissions.* Proceedings of the Combustion Institute, 2007. **31 I**: p. 77-98.
70. Johansen, J.M., et al., *Release of K, Cl, and S during combustion and co-combustion with wood of high-chlorine biomass in bench and pilot scale fuel beds.* Proceedings of the Combustion Institute, 2013. **34**(2): p. 2363-2372.

71. Knudsen, J.N., P.A. Jensen, and K. Dam-Johansen, *Transformation and release to the gas phase of Cl, K, and S during combustion of annual biomass.* Energy and Fuels, 2004. **18**(5): p. 1385-1399.
72. Pommer, L., et al., *Mechanisms behind the positive effects on bed agglomeration and deposit formation combusting forest residue with peat additives in fluidized beds.* Energy and Fuels, 2009. **23**(9): p. 4245-4253.
73. Ferrer, E., et al., *Fluidized bed combustion of refuse-derived fuel in presence of protective coal ash.* Fuel Processing Technology, 2005. **87**(1): p. 33-44.
74. Knudsen, J.N., et al., *Secondary capture of chlorine and sulfur during thermal conversion of biomass.* Energy and Fuels, 2005. **19**(2): p. 606-617.
75. Wei, X., et al., *Assessment of chlorine-alkali-mineral interactions during co-combustion of coal and straw*. Energy and Fuels, 2002. **16**(5): p. 1095-1108.
76. Müller, M., et al., *Release of K, Cl, and S species during co-combustion of coal and straw.* Energy and Fuels, 2006. **20**(4): p. 1444-1449.
77. Wu, H., et al., *Release and transformation of inorganic elements in combustion of a high-phosphorus fuel.* Energy and Fuels, 2011. **25**(7): p. 2874-2886.
78. Yue, M., Y. Wang, and X. Li, *Experimental study on the release characteristics of chlorine and alkali metal during co-firing of wheat straw and lean coal*, 2012. p. 3799-3802.
79. Cullis, C.F. and M.F.R. Mulcahy, *The kinetics of combustion of gaseous sulphur compounds.* Combustion and Flame, 1972. **18**(2): p. 225-292.
80. Glarborg, P. and P. Marshall, *Oxidation of reduced sulfur species: Carbonyl sulfide.* International Journal of Chemical Kinetics, 2013. **45**(7): p. 429-439.
81. Christensen, K.A. and H. Livbjerg, *A field study of submicron particles from the combustion of straw.* Aerosol Science and Technology, 1996. **25**(2): p. 185-199.
82. Alkemade, U. and K.H. Homann, *Gas-Phase Dimerization of Sodium Halides and Formation of Mixed Sodium/Phenyl Iodides.* Berichte der Bunsengesellschaft für physikalische Chemie, 1989. **93**(4): p. 434-439.
83. Blomberg, T., *A thermodynamic study of the gaseous potassium chemistry in the convection sections of biomass fired boilers.* Materials and Corrosion, 2011. **62**(7): p. 635-641.
84. Sengeløv, L.W., et al., *Sulfation of condensed potassium chloride by SO2.* Energy and Fuels, 2013. **27**(6): p. 3283-3289.
85. Lindberg, D., R. Backman, and P. Chartrand, *Thermodynamic evaluation and optimization of the (Na2SO4 + K2SO4 + Na2S2O7 + K2S2O7) system.* Journal of Chemical Thermodynamics, 2006. **38**(12): p. 1568-1583.
86. Steinberg, M. and K. Schofield, *The controlling chemistry of surface deposition from sodium and potassium seeded flames free of sulfur or chlorine impurities.* Combustion and Flame, 2002. **129**(4): p. 453-470.
87. Schofield, K. and M. Steinberg, *Sodium/sulfur chemical behavior in fuel-rich and -lean flames.* The Journal of Physical Chemistry, 1992. **96**(2): p. 715-726.
88. Steinberg, M. and K. Schofield, *The chemistry of sodium with sulfur in flames.* Progress in Energy and Combustion Science, 1990. **16**(4): p. 311-317.
89. Boonsongsup, L., K. Iisa, and W.J. Frederick Jr, *Kinetics of the Sulfation of NaCl at Combustion Conditions.* Industrial and Engineering Chemistry Research, 1997. **36**(10): p. 4212-4216.
90. Christensen, K.A. and H. Livbjerg, *A plug flow model for chemical reactions and aerosol nucleation and growth in an alkali-containing flue gas.* Aerosol Science and Technology, 2000. **33**(6): p. 470-489.
91. Hynes, A.J., M. Steinberg, and K. Schofield, *The chemical kinetics and thermodynamics of sodium species in oxygen-rich hydrogen flames.* The Journal of Chemical Physics, 1983. **80**(6): p. 2585-2597.
92. Jensen, D.E., *Alkali-metal compounds in oxygen-rich flames. A reinterpretation of experimental results.* Journal of the Chemical Society, Faraday Transactions 1: Physical Chemistry in Condensed Phases, 1982. **78**(9): p. 2835-2842.

93. Jensen, D.E. and G.A. Jones, *Kinetics of flame inhibition by sodium.* Journal of the Chemical Society, Faraday Transactions 1: Physical Chemistry in Condensed Phases, 1982. **78**(9): p. 2843-2850.
94. Jensen, D.E., G.A. Jones, and A.C.H. Mace, *Flame inhibition by potassium.* Journal of the Chemical Society, Faraday Transactions 1: Physical Chemistry in Condensed Phases, 1979. **75**: p. 2377-2385.
95. Birchall, J.D., *On the mechanism of flame inhibition by alkali metal salts.* Combustion and Flame, 1970. **14**(1): p. 85-95.
96. Bulewicz, E.M. and B.J. Kucnerowicz-Polak, *The action of sodium bicarbonate and of silica powder on upward propagating flame in a vertical duct.* Combustion and Flame, 1987. **70**(2): p. 127-135.
97. Dewitte, M., J. Vrebosch, and A. van Tiggelen, *Inhibition and extinction of premixed flames by dust particles.* Combustion and Flame, 1964. **8**(4): p. 257-266.
98. Dodding, R.A., R.F. Simmons, and A. Stephens, *The extinction of methane-air diffusion flames by sodium bicarbonate powders.* Combustion and Flame, 1970. **15**(3): p. 313-315.
99. Friedman, R. and J.B. Levy, *Inhibition of opposed-jet methane-air diffusion flames. The effects of alkali metal vapours and organic halides.* Combustion and Flame, 1963. **7**(1): p. 195-201.
100. Kim, H.T. and J.J. Reuther, *Temperature dependence of dry chemical premixed flame inhibition effectiveness.* Combustion and Flame, 1984. **57**(3): p. 313-317.
101. Rosser Jr, W.A., S.H. Inami, and H. Wise, *The effect of metal salts on premixed hydrocarbon-air flames.* Combustion and Flame, 1963. **7**(1): p. 107-119.
102. Sridhar Iya, K., S. Wollowitz, and W.E. Kaskan, *The mechanism of flame inhibition by sodium salts.* Symposium (International) on Combustion, 1975. **15**(1): p. 329-336.
103. Wei, X., et al., *Interactions of CO, HCl, and SOx in pulverised coal flames.* Fuel, 2004. **83**(9): p. 1227-1233.
104. Hindiyarti, L., et al., *Influence of potassium chloride on moist CO oxidation under reducing conditions: Experimental and kinetic modeling study.* Fuel, 2006. **85**(7-8): p. 978-988.
105. Roesler, J.F., R.A. Yetter, and F.L. Dryer, *Detailed kinetic modeling of moist CO oxidation inhibited by trace quantities of HCl.* Combustion science and technology, 1992. **85**(1-6): p. 1-22.
106. Roesler, J.F., R.A. Yetter, and F.L. Dryer, *Kinetic interactions of CO, NOx, and HCI emissions in postcombustion gases.* Combustion and Flame, 1995. **100**(3): p. 495-504.
107. Roesler, J.F., R.A. Yetter, and F.L. Dryer, *Inhibition and oxidation characteristics of chloromethanes in reacting CO/H2O/O2 mixtures.* Combustion science and technology, 1996. **120**(1-6): p. 11-37.
108. Mueller, C., P. Kilpinen, and M. Hupa, *Influence of HCl on the homogeneous reactions of CO and NO in postcombustion conditions - A kinetic modeling study.* Combustion and Flame, 1998. **113**(4): p. 579-588.
109. Glarborg, P. and P. Marshall, *Mechanism and modeling of the formation of gaseous alkali sulfates.* Combustion and Flame, 2005. **141**(1-2): p. 22-39.
110. Zamansky, V.M., et al., *Reactions of sodium species in the promoted SNCR process.* Combustion and Flame, 1999. **117**(4): p. 821-831.
111. Zamansky, V.M., et al., *Promotion of selective non-catalytic reduction of NO by sodium carbonate.* Symposium (International) on Combustion, 1998. **1**: p. 1443-1449.
112. Wei, X., et al., *The effect of HCl and SO2 on NOx formation in coal flames.* Energy and Fuels, 2003. **17**(5): p. 1392-1398.
113. Kassman, H., L. Bäfver, and L.E. Åmand, *The importance of SO2 and SO3 for sulphation of gaseous KCl - An experimental investigation in a biomass fired CFB boiler.* Combustion and Flame, 2010. **157**(9): p. 1649-1657.